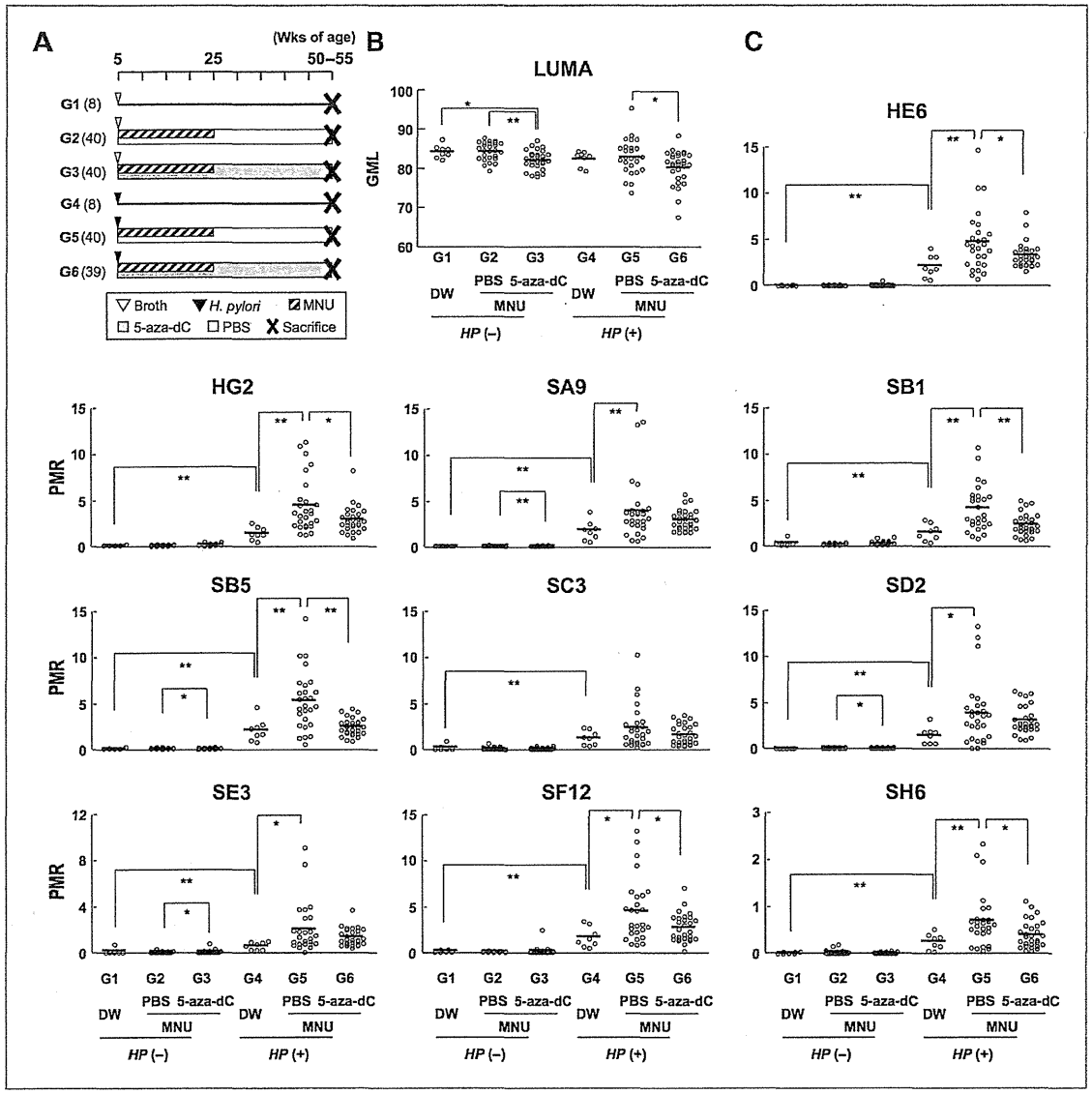

Figure 1. Suppression of DNA methylation by 5-aza-dC treatment. A, design of the carcinogenicity experiment. The number of animals is shown in parentheses. B, global DNA methylation levels analyzed by LUMA in GECs. C, methylation levels of 10 CGIs analyzed by qMSP in GECs. Both preexisting methylation and induction of aberrant methylation were suppressed by 5-aza-dC treatment. Bold horizontal bar, the average. *, $P < 0.05$; **, $P < 0.01$.

methylated fragments of a target CGI in *SssI*-treated DNA)/(number of the B2 repeat in *SssI*-treated DNA)] × 100.

Gene expression analyses

The number of cDNA molecules was quantified by quantitative reverse transcriptase-PCR (qRT-PCR) using gene-specific primers (*Il1b*, *Nos2*, and *Tnf*) as described (14). The number of cDNA molecules of a target gene was normalized to that of *Gapdh*.

Genomic PCR and sequencing

A forward primer (5′-AGATTCCTTGATGCCTGGGTGTC-3′) was designed in a region of the mouse *Tnf* promoter highly conserved with the human corresponding region. A reverse primer (5′-AGATTCCTTGATGCCTGGGTGTC-3′) was designed on the gerbil *Tnf* mRNA sequence (AB177841). The gerbil *Tnf* promoter was amplified using these primers, and the PCR product was directly sequenced with the same primers. The obtained sequence was

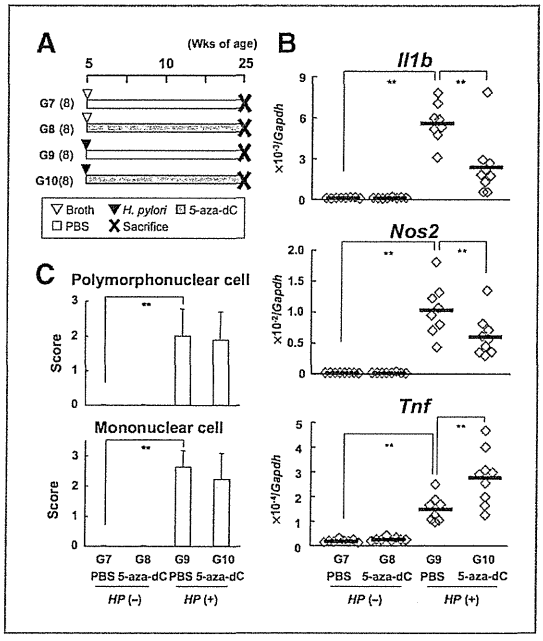

Figure 2. Dysregulation of inflammatory responses by 5-aza-dC treatment. A, design of the experiment for analysis of gastritis. The number of animals is shown in parentheses. B, expression levels of inflammation-related genes in gastric tissues containing submucosal layers. Bold horizontal bar indicates the average. C, infiltration score of polymorphonuclear cells and mononuclear cells in the stomach. Although the degree of *H. pylori*–induced infiltration of polymorphonuclear and mononuclear cells was not affected by 5-aza-dC treatment, expression of *Il1b* and *Nos2* was downregulated and that of *Tnf* was upregulated. Mean and SD are shown. **, $P < 0.01$.

registered in GenBank (AB762083.1). A CGI was searched by a EMBOSS CpG report program (40).

Statistical analysis

Statistical analyses were conducted by SPSS 13.0J (SPSS Japan Inc.). To evaluate significant difference between 2 independent groups of sample data, a Mann–Whitney *U* test was used. The difference of the proportion between 2 groups was evaluated by Fisher exact test.

Results

Suppression of *H. pylori*/MNU-induced gastric carcinogenesis by 5-aza-dC

To evaluate cancer prevention effects of 5-aza-dC, a carcinogenicity experiment was carried out (Fig. 1A). Among the gerbils with MNU treatment and *H. pylori* infection (G5 and G6), 5-aza-dC treatment decreased incidence of gastric cancers from 55.2% (G5) to 23.3% (G6, $P < 0.05$; Table 1). The incidence in G6 was similar to that in MNU-treated gerbils without *H. pylori* infection (G2, 20.7%). There were no significant differences in the tumor multiplicity and size among the groups. These results clearly showed that 5-aza-dC treatment suppressed *H. pylori*/MNU-induced gastric carcinogenesis in gerbils and suggested that it might have completely abrogated the cancer promotion effects of *H. pylori* infection. Among the MNU-treated gerbils without *H. pylori* infection (G2 and G3), 5-aza-dC treatment tended to decrease incidence of gastric cancers but it was not statistically significant.

Regardless of 5-aza-dC treatment, gerbils with MNU treatment (G2, G3, G5, and G6) showed low body weight than the gerbils without MNU treatment (G1 and G4), showing that the body weight loss was dependent upon MNU treatment, not upon 5-aza-dC treatment (Supplementary Fig. S2). Survival rates started to decrease from 25 weeks of age, and the decrease was dependent upon MNU treatment, not upon 5-aza-dC treatment (Supplementary Fig. S3). This showed that the dose of 5-aza-dC used in this study (125 μg/kg body weight) had no obvious effects on body weight and survival of gerbils.

Reduction of DNA methylation levels in GECs by 5-aza-dC

To confirm the demethylating effects of 5-aza-dC *in vivo*, methylation analyses were conducted in GECs. First, the global DNA methylation level was measured by LUMA, in which global CCGG methylation was measured by using

Table 1. Suppression of gastric cancers by 5-aza-dC

		Adenocarcinoma						
Group	Effective number	Well-differentiated	Poorly differentiated	Multiplicity (mean ± SD)	Diameter (mean ± SD), mm	Incidence (%)	Adenoma	Sarcoma
G1. *HP*(–) + DW	8	0	0	0	–	0/8 (0)	0	0
G2. *HP*(–) + MNU + PBS	29	3	3	1.0 ± 0	6.3 ± 1.6	6/29 (20.7)	1	2
G3. *HP*(–) + MNU + 5-aza-dC	33	0	2	1.0 ± 0	3.3 ± 3.3	2/33 (6.1)	1	0
G4. *HP*(+) + DW	8	0	0	0	–	0/8 (0)	0	0
G5. *HP*(+) + MNU + PBS	29	15	1	1.1 ± 0.3	5.7 ± 2.7	16/29 (55.2)[a]	0	2
G6. *HP*(+) + MNU + 5-aza-dC	30	4	3	1.0 ± 0	4.8 ± 1.7	7/30 (23.3)[b]	0	2

NOTE: 5-Aza-dC treatment decreased incidence of gastric cancers (adenocarcinomas) from 55.2% (G5) to 23.3% (G6).
[a]$P < 0.05$ compared with G3.
[b]$P < 0.05$ compared with G5.

a combination of methylation-sensitive and -insensitive restriction enzymes and pyrosequencing. Among the gerbils with MNU treatment and *H. pylori* infection (G5 and G6), 5-aza-dC treatment decreased the global methylation level from 83.0% ± 4.5% (mean ± SD)% (G5) to 80.3% ± 4.4% (G6, $P < 0.05$; Fig. 1B). Among the MNU-treated gerbils without *H. pylori* infection (G2 and G3), the methylation level was decreased by 5-aza-dC treatment (from 84.4% ± 2.3% in G2 to 82.2% ± 2.4% in G3, $P < 0.05$). No significant influence of *H. pylori* infection or MNU treatment was observed. These results indicated that 5-aza-dC worked as a DNA demethylating agent *in vivo* and decreased global methylation levels in GECs.

Next, methylation of 10 CGIs, where *H. pylori* infection was previously shown to induce aberrant methylation (Supplementary Fig. S1; refs. 14, 41), was analyzed by quantitative methylation-specific PCR (qMSP). 5-Aza-dC treatment reduced methylation levels in G6 to 46% to 80% of those in G5 for 6 CGIs (HE6, HG2, SB1, SB5, SF12, and SH6; $P < 0.05$; Fig. 1C). These results showed that 5-aza-dC treatment suppressed methylation induction by *H. pylori* infection and MNU treatment in GECs. The methylation levels in G5 were higher than those in G4 whereas those in G2 were not elevated compared with those in G1, indicating that MNU treatment had an augmenting effect on *H. pylori*–induced aberrant methylation.

Dysregulation of inflammation-related genes by 5-aza-dC

Among 10 inflammation-related genes whose expression was examined in the stomach, expression of 3 genes (*Il1b*, *Nos2*, and *Tnf*) has been shown to be associated with induction of methylation in GECs (14, 41). Therefore, we examined whether 5-aza-dC treatment affected expression of these 3 genes in the stomach after *H. pylori* infection using *H. pylori*–infected and -uninfected gerbils without MNU treatment (Fig. 2A). In the *H. pylori*–infected gerbils with 5-aza-dC treatment (G10), expression levels of *Il1b* and *Nos2* decreased to 42% and 58%, respectively ($P < 0.01$, respectively), of those in *H. pylori*–infected gerbils without 5-aza-dC treatment (G9; Fig. 2B). In contrast, *Tnf* was upregulated to 187% of G9 ($P < 0.01$). These results indicated that 5-aza-dC treatment caused up- and downregulation, namely dysregulation, of inflammation-related genes. As there was a possibility that upregulation of *Tnf* was due to demethylation of its promoter CGI, we sequenced its promoter region but found that there was no CGI (Supplementary Fig. S4). Because methylation of only promoters with CGIs can consistently silence their downstream genes (42), we considered that the upregulation of *Tnf* was unlikely to be due to demethylation by 5-aza-dC.

We also analyzed infiltration of inflammatory cells in the stomach. In gerbils with *H. pylori* infection (G9 and G10), 5-aza-dC treatment did not affect infiltration of mononuclear cells and polymorphonuclear cells (Fig. 2C). In gerbils without *H. pylori* infection (G7 and G8), there was little mononuclear cell and polymorphonuclear cell infiltration, and no effect of 5-aza-dC treatment was observed. These results showed that 5-aza-dC treatment did not affect infiltration of inflammatory cells.

Extra-gastric effects of 5-aza-dC treatment

To evaluate possible adverse effects of 5-aza-dC treatment, we first conducted macroscopic analysis. Although most organs did not show any abnormality, the testes were prominently atrophic in 5-aza-dC–treated gerbils [0.47 ± 0.05 (mean ± SD) g/2 testes in G3 and 0.50 ± 0.05 g/2 testes in G6] compared with gerbils in other groups (1.10 ± 0.11 g/2 testes in G2 and 1.09 ± 0.13 g/2 testes in G5).

We then conducted analysis of histopathologic abnormalities and global DNA methylation levels in the testes, small intestine, liver, and kidneys. In the testes of 5-aza-dC–treated gerbils, the numbers of spermatozoa and spermatids were markedly decreased regardless of *H. pylori*

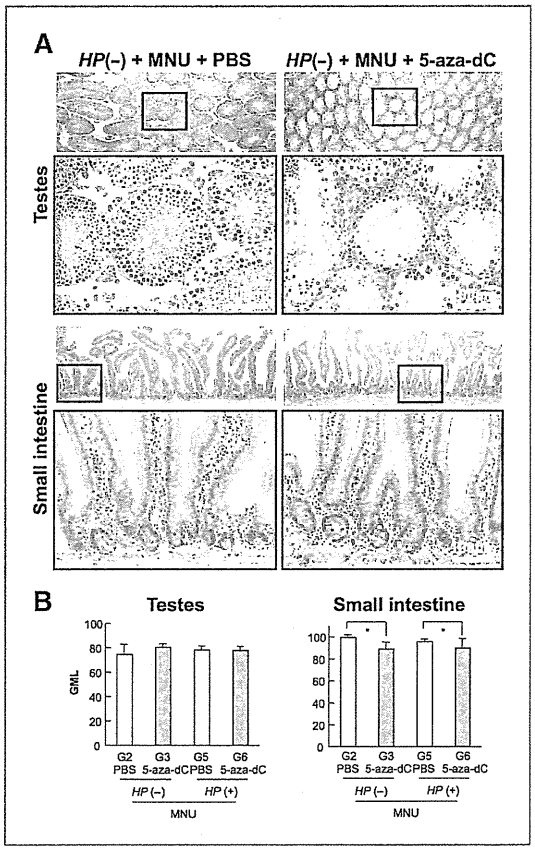

Figure 3. Adverse effects of 5-aza-dC treatment in extra-gastric tissues. A, tissue sections of the testes and small intestine. Bottom, is a magnified view of the region in the black rectangle in the top. Numbers of spermatozoa and spermatids were markedly decreased in the testes of 5-aza-dC–treated gerbil. B, global methylation levels in the testes and small intestine. Five gerbils in each group were randomly selected, and the methylation levels were measured by LUMA. Mean and SD are shown. *, $P < 0.05$. By 5-aza-dC-treatment, the global methylation level did not decrease in the testes but did in the small intestine.

infection status (Fig. 3A). Despite the presence of hypospermatogenesis, there was no significant decrease of the global methylation level (Fig. 3B). In contrast, in the small intestine, the global methylation level was reduced by 10.4% and 5.6% (G3 and G6, respectively Fig. 3B). However, no histologic changes compared with the untreated gerbils were observed (Fig. 3A). As for the liver and kidneys, there were no histologic abnormalities or reduction of global methylation levels in G3 and G6 (Supplementary Fig. S5).

Discussion

Our study using a gerbil model showed that 5-aza-dC treatment suppressed *H. pylori*/MNU-induced gastric cancers. This study showed for the first time that chemoprevention using a DNA demethylating agent is effective for chronic inflammation–associated cancers. As chronic inflammation contributes to about 25% of all cancer cases (43), and aberrant DNA methylation is frequently observed in tissues exposed to chronic inflammation (29), suppression of aberrant methylation might become an effective preventive approach for these types of cancers. This study also showed that induction of aberrant methylation is an important mechanism for gastric carcinogenesis by *H. pylori* infection.

As mechanisms of suppression of gastric cancers by 5-aza-dC, at least 2 modes of action were present. The first one was the DNA demethylating effect. 5-Aza-dC treatment decreased global methylation level in GECs and suppressed hypermethylation of CGIs. These results suggested that 5-aza-dC was capable of removing aberrant DNA methylation induced by *H. pylori* infection and thereby prevented cancer development. The second one was the effect on inflammation. It was previously shown that inflammation triggered by *H. pylori* infection is pivotal for aberrant methylation induction, and expression of inflammation-related genes (*Il1b*, *Nos2*, and *Tnf*) in the stomach is associated with the induction (14, 41). The present study showed that 5-aza-dC treatment dysregulated expression of these genes. Therefore, there is a possibility that altered balances among the related cytokines might have led to the reduced methylation induction.

Recently, in the stomach of hypergastrinemic INS-GAS mice, inhibition of *H. pylori* (*H. felis*)-induced global demethylation by folic acid supplementation was reported to suppress gastric dysplasia (44). The data are seemingly discordant with our data showing a cancer preventive effect by DNA demethylation. However, in the INS-GAS mice, global hypomethylation by *H. felis* was evident, suggesting that the demethylation plays important roles in the carcinogenesis. Hypermethylation by folic acid might exert the cancer preventive effect via suppression of global demethylation. In contrast, in our gerbil study, hypermethylation of CGIs by *H. pylori* infection, rather than global demethylation, was evident, suggesting that hypermethylation of CGIs rather than global demethylation was the major mechanism for the carcinogenesis. Thus, demethylation by 5-aza-dC was considered to have exerted the preventive effect via suppression of hypermethylation of CGIs.

No obvious adverse effect of 5-aza-dC treatment was observed besides hypospermatogenesis in the testes. Hypospermatogenesis due to 5-aza-dC treatment was reported in mice (24). As global hypomethylation was not detected in the testes of the 5-aza-dC–treated gerbils, the effect was speculated to be independent of its DNA demethylating activity. However, we cannot exclude the possibility that decrease of methylation was not detected due to immediate elimination of spermatozoa/spermatids with decreased DNA methylation. Regardless of the mechanism, the presence of this adverse effect precludes 5-aza-dC as a chemoprevention agent for the general population. However, chemoprevention by a DNA demethylating agent itself still might become a promising strategy if a DNA demethylating agent without such toxicity is developed.

Demethylating effects by 5-aza-dC were observed in the stomach and the small intestine, but not in the liver and the kidneys. Specific global demethylation in the stomach and intestine was also observed in the female $Apc^{min/+}$ mice administered a demethylating agent, zebularine (23). Turnover of epithelial cells in these tissues is known to be very rapid, being 3 to 4 days in mice (45, 46). As demethylating effects of 5-aza-dC and zebularine are exerted after their incorporation into gDNA and DNA replication, rapid cell turnover in the stomach and intestine could explain the organ-specific global demethylation.

Individuals with a severe epigenetic field defect, in contrast with the general population, can be considered as a target population for cancer prevention using 5-aza-dC after careful balancing of its preventive and adverse effects. In the case of gastric cancers, eradication of *H. pylori* is the primary strategy for prevention (47), but the incidence of gastric cancers remains high, even after *H. pylori* eradication, especially in persons with intestinal metaplasia and gastric atrophy (48). Notably, aberrant methylation in gastric mucosae decreases by *H. pylori* eradication, but it does not disappear completely (14, 49). The level of the remaining methylation reflects the risk of gastric cancers (8, 9). As DNA demethylating agents are likely to remove such accumulated methylation and suppress gastric cancers development, these individuals with a severe epigenetic field defect may benefit from epigenetic chemoprevention.

In summary, treatment with 5-aza-dC effectively prevented gastric cancers induced by *H. pylori* infection in gerbils, suppressed DNA methylation in GECs, and induced dysregulation of inflammation. Chemoprevention with a DNA demethylating agent is expected to become an effective strategy for prevention of chronic inflammation–associated cancers.

Disclosure of Potential Conflicts of Interest

No potential conflicts of interest were disclosed.

Authors' Contributions

Conception and design: T. Niwa, M. Tatematsu, T. Ushijima
Development of methodology: T. Niwa, T. Tsukamoto
Acquisition of data (provided animals, acquired and managed patients, provided facilities, etc.): T. Niwa, T. Toyoda
Analysis and interpretation of data (e.g., statistical analysis, biostatistics, computational analysis): T. Niwa, T. Toyoda
Writing, review, and/or revision of the manuscript: T. Niwa, T. Ushijima
Administrative, technical, or material support (i.e., reporting or organizing data, constructing databases): A. Mori
Study supervision: M. Tatematsu

Acknowledgments

The authors thank Ms. R. Shimada (Qiagen K.K.) for her technical support of LUMA.

Grant Support

This study was supported by Grants-in-Aid for The Third-term Comprehensive Cancer Control Strategy from the Ministry of Health, Labour, and Welfare, Japan (T. Ushijima); Grants-in-Aid for Young Scientists (#23701114) from the Japan Society for the Promotion of Science (T. Niwa); and Grants-in-Aid from the Foundation of Promotion of Cancer Research, Japan (T. Niwa).

The costs of publication of this article were defrayed in part by the payment of page charges. This article must therefore be hereby marked *advertisement* in accordance with 18 U.S.C. Section 1734 solely to indicate this fact.

Received August 29, 2012; revised December 19, 2012; accepted January 8, 2013; published online April 4, 2013.

References

1. Taby R, Issa JP. Cancer epigenetics. CA Cancer J Clin 2010;60:376–92.
2. Howard G, Eiges R, Gaudet F, Jaenisch R, Eden A. Activation and transposition of endogenous retroviral elements in hypomethylation induced tumors in mice. Oncogene 2008;27:404–8.
3. Esteller M. Epigenetics in cancer. N Engl J Med 2008;358:1148–59.
4. Jones PA, Baylin SB. The epigenomics of cancer. Cell 2007;128:683–92.
5. Hsieh CJ, Klump B, Holzmann K, Borchard F, Gregor M, Porschen R. Hypermethylation of the p16INK4a promoter in colectomy specimens of patients with long-standing and extensive ulcerative colitis. Cancer Res 1998;58:3942–5.
6. Issa JP, Ahuja N, Toyota M, Bronner MP, Brentnall TA. Accelerated age-related CpG island methylation in ulcerative colitis. Cancer Res 2001;61:3573–7.
7. Kondo Y, Kanai Y, Sakamoto M, Mizokami M, Ueda R, Hirohashi S. Genetic instability and aberrant DNA methylation in chronic hepatitis and cirrhosis–A comprehensive study of loss of heterozygosity and microsatellite instability at 39 loci and DNA hypermethylation on 8 CpG islands in microdissected specimens from patients with hepatocellular carcinoma. Hepatology 2000;32:970–9.
8. Maekita T, Nakazawa K, Mihara M, Nakajima T, Yanaoka K, Iguchi M, et al. High levels of aberrant DNA methylation in *Helicobacter pylori*-infected gastric mucosae and its possible association with gastric cancer risk. Clin Cancer Res 2006;12:989–95.
9. Nakajima T, Maekita T, Oda I, Gotoda T, Yamamoto S, Umemura S, et al. Higher methylation levels in gastric mucosae significantly correlate with higher risk of gastric cancers. Cancer Epidemiol Biomarkers Prev 2006;15:2317–21.
10. Perri F, Cotugno R, Piepoli A, Merla A, Quitadamo M, Gentile A, et al. Aberrant DNA methylation in non-neoplastic gastric mucosa of H. Pylori infected patients and effect of eradication. Am J Gastroenterol 2007;102:1361–71.
11. Egan BJ, Holmes K, O'Connor HJ, O'Morain CA. *Helicobacter pylori* gastritis, the unifying concept for gastric diseases. Helicobacter 2007;12 Suppl 2:39–44.
12. Fox JG, Wang TC. Inflammation, atrophy, and gastric cancer. J Clin Invest 2007;117:60–9.
13. Moss SF, Blaser MJ. Mechanisms of disease: inflammation and the origins of cancer. Nat Clin Pract Oncol 2005;2:90–7.
14. Niwa T, Tsukamoto T, Toyoda T, Mori A, Tanaka H, Maekita T, et al. Inflammatory processes triggered by *Helicobacter pylori* infection cause aberrant DNA methylation in gastric epithelial cells. Cancer Res 2010;70:1430–40.
15. Blackburn EH, Tlsty TD, Lippman SM. Unprecedented opportunities and promise for cancer prevention research. Cancer Prev Res 2010;3:394–402.
16. Issa JP. Cancer prevention: epigenetics steps up to the plate. Cancer Prev Res (Phila) 2008;1:219–22.
17. Prevention of cancer in the next millennium: Report of the Chemoprevention Working Group to the American Association for Cancer Research. Cancer Res 1999;59:4743–58.
18. Greenwald P. Cancer chemoprevention. BMJ 2002;324:714–8.
19. Hursting SD, Slaga TJ, Fischer SM, DiGiovanni J, Phang JM. Mechanism-based cancer prevention approaches: targets, examples, and the use of transgenic mice. J Natl Cancer Inst 1999;91:215–25.
20. Issa JP, Kantarjian HM. Targeting DNA methylation. Clin Cancer Res 2009;15:3938–46.
21. Yoo CB, Jones PA. Epigenetic therapy of cancer: past, present and future. Nat Rev Drug Discov 2006;5:37–50.
22. Laird PW, Jackson-Grusby L, Fazeli A, Dickinson SL, Jung WE, Li E, et al. Suppression of intestinal neoplasia by DNA hypomethylation. Cell 1995;81:197–205.
23. Yoo CB, Chuang JC, Byun HM, Egger G, Yang AS, Dubeau L, et al. Long-term epigenetic therapy with oral zebularine has minimal side effects and prevents intestinal tumors in mice. Cancer Prev Res 2008;1:233–40.
24. McCabe MT, Low JA, Daignault S, Imperiale MJ, Wojno KJ, Day ML. Inhibition of DNA methyltransferase activity prevents tumorigenesis in a mouse model of prostate cancer. Cancer Res 2006;66:385–92.
25. Lantry LE, Zhang Z, Crist KA, Wang Y, Kelloff GJ, Lubet RA, et al. 5-Aza-2′-deoxycytidine is chemopreventive in a 4-(methyl-nitrosamino)-1-(3-pyridyl)-1-butanone-induced primary mouse lung tumor model. Carcinogenesis 1999;20:343–6.
26. Tang XH, Albert M, Scognamiglio T, Gudas LJ. A DNA methyltransferase inhibitor and all-trans retinoic acid reduce oral cavity carcinogenesis induced by the carcinogen 4-nitroquinoline 1-oxide. Cancer Prev Res 2009;2:1100–10.
27. Baba S, Yamada Y, Hatano Y, Miyazaki Y, Mori H, Shibata T, et al. Global DNA hypomethylation suppresses squamous carcinogenesis in the tongue and esophagus. Cancer Sci 2009;100:1186–91.
28. Belinsky SA, Klinge DM, Stidley CA, Issa JP, Herman JG, March TH, et al. Inhibition of DNA methylation and histone deacetylation prevents murine lung cancer. Cancer Res 2003;63:7089–93.
29. Niwa T, Ushijima T. Induction of epigenetic alterations by chronic inflammation and its significance on carcinogenesis. Adv Genet 2010;71:41–56.
30. Ushijima T. Epigenetic field for cancerization. J Biochem Mol Biol 2007;40:142–50.
31. Tatematsu M, Tsukamoto T, Mizoshita T. Role of *Helicobacter pylori* in gastric carcinogenesis: the origin of gastric cancers and heterotopic proliferative glands in Mongolian gerbils. Helicobacter 2005;10:97–106.
32. Tsukamoto T, Mizoshita T, Tatematsu M. Animal models of stomach carcinogenesis. Toxicol Pathol 2007;35:636–48.
33. Peterson AJ, Menheniott TR, O'Connor L, Walduck AK, Fox JG, Kawakami K, et al. *Helicobacter pylori* infection promotes methylation and silencing of trefoil factor 2, leading to gastric tumor development in mice and humans. Gastroenterology 2010;139:2005–17.
34. Shimizu N, Ikehara Y, Inada K, Nakanishi H, Tsukamoto T, Nozaki K, et al. Eradication diminishes enhancing effects of *Helicobacter pylori* infection on glandular stomach carcinogenesis in Mongolian gerbils. Cancer Res 2000;60:1512–4.

35. Cheng H, Bjerknes M, Amar J. Methods for the determination of epithelial cell kinetic parameters of human colonic epithelium isolated from surgical and biopsy specimens. Gastroenterology 1984;86:78–85.
36. Tatematsu M, Yamamoto M, Shimizu N, Yoshikawa A, Fukami H, Kaminishi M, et al. Induction of glandular stomach cancers in *Helicobacter pylori* -sensitive Mongolian gerbils treated with N-methyl-N-nitrosourea and N-methyl-N′-nitro-N-nitrosoguanidine in drinking water. Jpn J Cancer Res 1998;89:97–104.
37. Toyoda T, Tsukamoto T, Mizoshita T, Nishibe S, Deyama T, Takenaka Y, et al. Inhibitory effect of nordihydroguaiaretic acid, a plant lignan, on *Helicobacter pylori* -associated gastric carcinogenesis in Mongolian gerbils. Cancer Sci 2007;98:1689–95.
38. Karimi M, Johansson S, Ekstrom TJ. Using LUMA: a Luminometric-based assay for global DNA-methylation. Epigenetics 2006;1:45–8.
39. Yamashita S, Takahashi S, McDonell N, Watanabe N, Niwa T, Hosoya K, et al. Methylation silencing of transforming growth factor-beta receptor type II in rat prostate cancers. Cancer Res 2008;68:2112–21.
40. Rice P, Longden I, Bleasby A. EMBOSS: the European Molecular Biology Open Software Suite. Trends Genet 2000;16:276–7.
41. Hur K, Niwa T, Toyoda T, Tsukamoto T, Tatematsu M, Yang HK, et al. Insufficient role of cell proliferation in aberrant DNA methylation induction and involvement of specific types of inflammation. Carcinogenesis 2011;32:35–41.
42. Weber M, Hellmann I, Stadler MB, Ramos L, Paabo S, Rebhan M, et al. Distribution, silencing potential and evolutionary impact of promoter DNA methylation in the human genome. Nat Genet 2007;39:457–66.
43. Hussain SP, Harris CC. Inflammation and cancer: an ancient link with novel potentials. Int J Cancer 2007;121:2373–80.
44. Gonda TA, Kim YI, Salas MC, Gamble MV, Shibata W, Muthupalani S, et al. Folic acid increases global DNA methylation and reduces inflammation to prevent Helicobacter-associated gastric cancer in mice. Gastroenterology 2012;142:824–33.
45. Gavrieli Y, Sherman Y, Ben-Sasson SA. Identification of programmed cell death in situ via specific labeling of nuclear DNA fragmentation. J Cell Biol 1992;119:493–501.
46. Lee ER. Dynamic histology of the antral epithelium in the mouse stomach: III. Ultrastructure and renewal of pit cells. Am J Anat 1985;172:225–40.
47. Asaka M, Kato M, Takahashi S, Fukuda Y, Sugiyama T, Ota H, et al. Guidelines for the management of *Helicobacter pylori* infection in Japan: 2009 revised edition. Helicobacter 2010;15:1–20.
48. Kabir S. Effect of *Helicobacter pylori* eradication on incidence of gastric cancer in human and animal models: underlying biochemical and molecular events. Helicobacter 2009;14:159–71.
49. Nakajima T, Enomoto S, Yamashita S, Ando T, Nakanishi Y, Nakazawa K, et al. Persistence of a component of DNA methylation in gastric mucosae after *Helicobacter pylori* eradication. J Gastroenterol 2010; 45:37–44.

Carcinogenesis vol.33 no.12 pp.2384–2390, 2012
doi:10.1093/carcin/bgs294
Advance Access publication September 13, 2012

Induction of aberrant trimethylation of histone H3 lysine 27 by inflammation in mouse colonic epithelial cells

Hideyuki Takeshima, Daigo Ikegami, Mika Wakabayashi, Tohru Niwa, Young-Joon Kim[1] and Toshikazu Ushijima*

Division of Epigenomics, National Cancer Center Research Institute, 5-1-1 Tsukiji, Chuo-ku, 104-0045, Tokyo, Japan and [1]Department of Biochemistry, Genome Regulation Center, Yonsei University, Seoul, Korea

*To whom correspondence should be addressed. Fax: +81 3 5565 1753; Email: tushijim@ncc.go.jp

A field for cancerization (field defect), where genetic and epigenetic alterations are accumulated in normal-appearing tissues, is involved in human carcinogenesis, especially cancers associated with chronic inflammation. Although aberrant DNA methylation is involved in the field defect and induced by chronic inflammation, it is still unclear for trimethylation of histone H3 lysine 27 (H3K27me3), which is involved in gene repression independent of DNA methylation and functions as a pre-mark for aberrant DNA methylation. In this study, using a mouse colitis model induced by dextran sulfate sodium (DSS), we aimed to clarify whether aberrant H3K27me3 is induced by inflammation and involved in a field defect. ChIP-on-chip analysis of colonic epithelial cells revealed that H3K27me3 levels were increased or decreased for 266 genomic regions by aging, and more extensively (23 increased and 3574 decreased regions) by colitis. Such increase or decrease of H3K27me3 was induced as early as 2 weeks after the initiation of DSS treatment, and persisted at least for 16 weeks even after the inflammation disappeared. Some of the aberrant H3K27me3 in colonic epithelial cells was carried over into colon tumors. Furthermore, H3K27me3 acquired at *Dapk1* by colitis was followed by increased DNA methylation, supporting its function as a pre-mark for aberrant DNA methylation. These results demonstrated that aberrant H3K27me3 can be induced by exposure to a specific environment, such as colitis, and suggested that aberrant histone modification, in addition to aberrant DNA methylation, is involved in the formation of a field defect.

Introduction

A field for cancerization (field defect) is known as normal-appearing tissues predisposed to carcinogenesis, and is deeply involved in development of human cancers, especially those associated with chronic inflammation, such as gastric cancers (1). The predisposition is considered to be due to accumulation of genetic and epigenetic alterations (2,3). Although the frequencies of genetic alterations in normal-appearing tissues are too low to be accurately measured (4), high levels of aberrant DNA methylation can be present in normal-appearing tissues and the levels can be correlated with risk of cancer development (epigenetic field defect) (3). DNA methylation in normal-appearing tissues is now known to be induced by aging (5–7) and exposure to specific carcinogenic factors, represented by chronic inflammation (8–10).

Epigenetic modifications consist of not only DNA methylation but also histone modifications (11), which are involved in both gene repression and activation and have various biological functions (12,13). Among histone modifications, trimethylation of histone H3 lysine 27 (H3K27me3) is involved in gene repression, independently of DNA methylation (14). Aberrant H3K27me3 is frequently observed in various cancers (14–16), and is involved in repression of tumor-suppressor genes such as *CDH1* (E-cadherin) and *RUNX3* (17,18). H3K27me3 is also important as a pre-mark in normal cells of genes in which aberrant DNA methylation is induced during carcinogenesis (19–24). Nevertheless, in contrast with the clear involvement of aberrant DNA methylation in the formation of an epigenetic field defect, the involvement of aberrant histone modifications is currently unknown. In addition, although induction of aberrant H3K27me3 by cobalt compounds and cigarette smoke condensate has been reported in cultured cells (25,26), its inducers *in vivo* are unknown.

In this study, we aimed to clarify whether aberrant H3K27me3 is induced in normal-appearing tissues by exposure to a specific environment and can be involved in an epigenetic field defect. To this end, we used a mouse colitis model induced by dextran sulfate sodium (DSS) because we previously demonstrated that aberrant DNA methylation can be induced at an early stage in this model (27).

Abbreviations: CGI, CpG island; ChIP, chromatin immunoprecipitation; DSS, dextran sulfate sodium; FACS, fluorescence-activated cell sorting; H3K27me3, trimethylation of histone H3 lysine 27; qRT-PCR, quantitative reverse transcription-PCR.

Materials and methods

Animals and induction of inflammation and colon tumors

Male BALB/c mice were purchased from Charles River Laboratories (Yokohama, Japan). To induce colitis, 7-week-old mice were given DSS (molecular weight = 36 000–50 000; MP Biochemicals, Solon, OH) in drinking water at a concentration of 2.0% (wt/vol) for 1 week. To induce colon tumors, BALB/c mice were intraperitoneally injected with 10 mg/kg body weight of azoxymethane (NARD Institute, Amagasaki, Japan) and given DSS in drinking water (27), and tumors were obtained at 15 weeks after the initiation of DSS treatment. Colonic epithelial cells were isolated from distal large bowels by the crypt isolation technique (27). For the analysis of expression of inflammation-related genes, the entire colon, including both colonic mucosae and muscle layer, was used. All the animal experiments were approved by the Committee for Ethics in Animal Experimentation at the National Cancer Center.

Chromatin immunoprecipitation

As described previously (23), 10 µg of chromatin extracted from cross-linked colonic epithelial cells or colon tumor cells was immunoprecipitated by using 2 µg of specific antibodies [H3K27me3 (07-449, Millipore, Billerica, MA), H3K9me2 (308-32361, Wako, Osaka, Japan) and H3K9me3 (301-34833, Wako)] and Dynabeads Protein A (Invitrogen Dynal AS, Oslo, Norway). After reversal of cross-link, DNA was recovered with RNaseA and proteinase K treatment, followed by phenol/chloroform extraction and isopropanol precipitation. Recovered DNA was dissolved in 33 µl of 1 × TE (10 mM Tris-HCl and 1 mM ethylenediaminetetraacetic acid).

One microliter of immunoprecipitated and input DNA was used for real-time chromatin immunoprecipitation (ChIP)–quantitative PCR (ChIP-qPCR). ChIP-qPCR was performed as described (23) with primers listed in **Supplementary Table 1**, available at *Carcinogenesis* Online. The numbers of DNA molecules in input and immunoprecipitated samples were obtained by comparing its amplification curve with those of standard samples with known numbers of DNA molecules. The specificity of the ChIP assay was confirmed by using primers for control regions (**Supplementary Figure 1**, available at *Carcinogenesis* Online).

Microarray analysis

Five hundred nanograms of immunoprecipitated and input DNA were labeled with Cy5 and Cy3, respectively, and hybridized with a mouse CpG island (CGI) oligonucleotide microarray (Agilent Technologies, Santa Clara, CA). Microarray scanning and data processing were performed as described (23,28), and the obtained signal ratio [Cy5 signal (bound)/Cy3 signal (input)] was normalized by the median of signal ratios of all probes. The H3K27me3 level of a region was evaluated using the average of signal ratios of the probes within the region. Genomic regions were defined as an assembly of probes with intervals <500 bp, and a region spanning both a promoter and gene body was split into two regions. Regions with only one or two probes were excluded from the analysis, and 16 126 regions were analyzed. When H3K27me3 levels in two samples were compared, we selected regions that showed a decrease or increase of 1.5-fold or more and had H3K27me3 levels higher than 1.5 in at least one sample.

Fluorescence-activated cell sorting

Colonic epithelial cells obtained from three mice were incubated in Hanks' balanced salt solution containing 10 mM *N*-2-hydroxyethylpiperazine-*N'*-2-ethanesulfonic acid (pH 7.3), 1 mg/ml collagenase D (Roche Diagnostics, Penzberg, Germany) and 5 μg/ml DNase I (Sigma–Aldrich, St Louis, MO) at 37°C for 20 min with gentle agitation. Dispersed epithelial cells were treated with 1% formaldehyde at 30°C for 10 min and filtered with a cell strainer (BD, Franklin Lakes, NJ). The cross-linked cells were incubated with a phycoerythrin-labeled anti-mouse Epcam antibody (eBioscience, San Diego, CA) and a fluorescein isothiocyanate-labeled anti-Cd45 antibody (Miltenyi Biotech, Auburn, CA), and sorted using FACSAria II cell sorter (BD).

Quantitative reverse transcription-PCR

Total RNA was isolated using ISOGEN (Nippon Gene, Tokyo, Japan). cDNA was synthesized from 1 μg of total RNA using SuperScript III reverse transcriptase and an oligo $(dT)_{12-18}$ primer (Invitrogen, Carlsbad, CA). Quantitative reverse transcription-PCR (qRT-PCR) was performed as described (10) using primers listed in Supplementary Table 2, available at *Carcinogenesis* Online. The number of target cDNA molecules was normalized to that of *Gapdh* cDNA molecules.

Quantitative methylation-specific PCR

One microgram of *Bam*HI-digested genomic DNA was treated with sodium bisulfite as described (29). Bisulfite-treated DNA was re-suspended in 40 μl of 1 × TE, and 1 μl was used for quantitative methylation-specific PCR using primers specific to methylated target loci and to B2 SINE repeat (Supplementary Table 3, available at *Carcinogenesis* Online). DNA methylation levels were expressed as the percentage of methylation reference (27,30). Percentage of methylation reference was calculated as [(number of molecules methylated at a target region in a sample)/(number of B2 SINE repeat in the sample)]/[(number of molecules methylated at the target region in fully methylated DNA)/(number of B2 SINE repeat in the fully methylated DNA)] × 100. Genomic DNA treated with *SssI* methylase (New England Biolabs, Beverly, MA) was used as fully methylated DNA.

Results

Alterations of H3K27me3 levels were induced by aging, and more extensively by colitis

First, age-associated alterations of H3K27me3 levels were searched for by ChIP-CGI microarray (ChIP-on-chip) analysis of colonic epithelial cells obtained from 7-week-old mice and those from 23-week-old mice (Figure 1A and 1B). Among the 16 126 regions analyzed, H3K27me3 levels of 243 and 23 regions were increased and decreased, respectively. Then, colitis-associated alterations of H3K27me3 levels were searched for by comparing H3K27me3 levels between colonic epithelial cells of 23-week-old mice exposed to DSS-induced colitis and those of age-matched mock-treated mice (Figure 1A and 1C). H3K27me3 levels of 27 and 3782 regions were increased and decreased, respectively, by colitis. Among the 3809 regions with alterations, 212 regions overlapped with those whose alterations were induced by aging (Figure 1D). For the remaining 3597 regions, H3K27me3 levels of 23 (including 7 promoters and 15 gene bodies) and 3574 (including 866 promoters and 1934 gene bodies) regions were increased and decreased, respectively (Figure 1E).

The data obtained by ChIP-on-chip analysis were confirmed by ChIP-qPCR using 21 regions with H3K27me3-level alterations of 1.5-fold or more and four regions with alterations of 1.5-fold or less (Supplementary Table 4, available at *Carcinogenesis* Online). Alterations of the H3K27me3 levels obtained by both methods were well correlated ($r = 0.71$, Supplementary Figure 2, available at *Carcinogenesis* Online). These results showed that most alterations in H3K27me3 levels detected by ChIP-on-chip could be confirmed by ChIP-qPCR, and such alterations could be induced by exposure to colitis.

Since H3K27me3 alterations were extensive, we analyzed alterations of other well-known repressive histone modifications, H3K9me2 and H3K9me3 (12). As with the case of H3K27me3, large numbers of regions showed alterations of these two modifications (Supplementary Figure 3A–D, available at *Carcinogenesis* Online). Notably, regions with H3K27me3-level alterations hardly overlapped with regions with either H3K9me2- or H3K9me3-level alterations (Supplementary Figure 3E and F, available at *Carcinogenesis* Online).

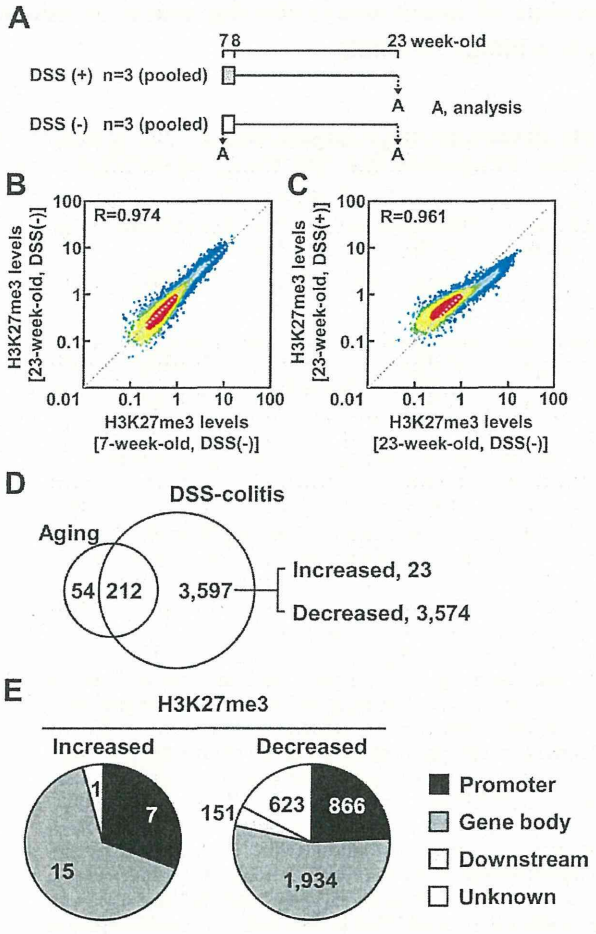

Fig. 1. Identification of genomic regions whose H3K27me3 levels were altered by aging and exposure to DSS-induced colitis. (**A**) Experimental protocol of sample preparation for ChIP-on-chip. (**B**) Alterations of the H3K27me3 levels in colonic epithelial cells by aging. Among the 16 126 regions analyzed, H3K27me3 levels of 243 and 23 regions were increased and decreased, respectively, at 1.5-fold or more by aging. (**C**) Alterations of the H3K27me3 levels by colitis. H3K27me3 levels of 27 and 3782 regions were increased and decreased, respectively, at 1.5-fold or more. (**D**) The overlap of regions whose H3K27me3 levels were altered by aging and those by colitis. Among the 3597 regions specifically altered by colitis, 23 and 3574 regions showed increased and decreased, respectively, H3K27me3 levels. (**E**) Classification of regions with H3K27me3-level alterations. Regions were classified into promoter (within 10 kb upstream of the transcription start site), gene body and downstream (within 10 kb downstream from genes) regions. Twenty-three regions with increased H3K27me3 levels contained 7 promoters and 15 gene bodies, respectively, and 3574 regions with decreased H3K27me3 levels contained 866 promoters and 1934 gene bodies, respectively. Regions that could not be classified by these criteria are indicated as unknown.

Aberrant H3K27me3 was induced at early stage, and remained for a long term even after its inducer disappeared

The temporal profiles of H3K27me3 levels in the course of DSS treatment were analyzed using 10 regions that showed alterations of 2-fold or more by ChIP-qPCR (Figure 2A). Among the six regions whose H3K27me3 levels were increased at 16 weeks (23-week-old mice) from the initiation of DSS treatment, three regions (*Abca1*, *Dapk1* and *Gramd1b*) showed significant increase of H3K27me3 levels at 2 weeks (Figure 2B). Similarly, among the four regions whose H3K27me3 levels were decreased at 16 weeks, two regions [*B4galnt1* (CGI2300) and *Plcd3*] showed significant decrease of H3K27me3 levels at 2

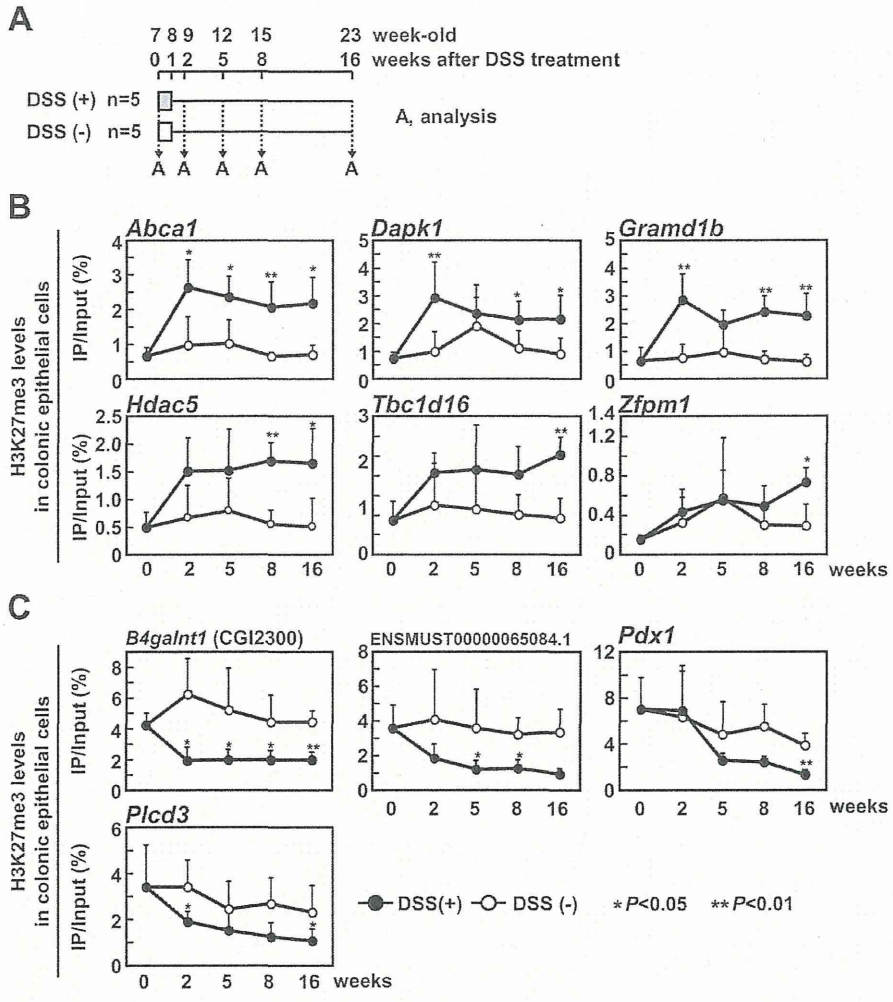

Fig. 2. Temporal profiles of H3K27me3 levels in the course of DSS-induced colitis. (**A**) Experimental protocol of preparation of colonic epithelial cells for ChIP-qPCR. (**B**) Analysis of genomic regions with increased H3K27me3. H3K27me3 levels of *Abca1*, *Dapk1* and *Gramd1b* were significantly increased at 2 weeks, and alterations persisted for at least 16 weeks, whereas those of *Hdac5*, *Tbc1d16* and *Zfpm1* were significantly increased only at late phases of colitis. Black and white circles show DSS-treated ($n = 5$) and mock-treated ($n = 5$) groups, respectively. The significance of difference was evaluated by the Mann–Whitney *U*-test (*$P < 0.05$, **$P<0.01$). (**C**) Analysis of genomic regions with decreased H3K27me3. H3K27me3 levels of *B4galnt1* (CGI2300) and *Plcd3* were significantly decreased at 2 weeks, and alterations persisted at least for 16 weeks. Those of ENSMUST00000065084.1 and *Pdx1* were significantly decreased only at late phase of colitis.

weeks (Figure 2C). Alterations in the H3K27me3 levels in these regions persisted at least until 16 weeks. Similar alterations in the H3K27me3 levels were confirmed in fluorescence-activated cell sorting (FACS)-purified colonic epithelial cells (Supplementary Figure 4, available at *Carcinogenesis* Online).

Temporal profiles of inflammation were then analyzed by examining expression of inflammation-related genes, *Il1b*, *Nos2* and *Tnf*, which are known to be upregulated in DSS-induced mouse colitis (27). Although the three genes were significantly upregulated at 2 and 5 weeks, their upregulation disappeared at 8 and 16 weeks (Figure 3A). Temporal profiles of expression of genes involved in the regulation of H3K27me3 were then analyzed. Expression levels of components of PRC2 (*Ezh2*, *Eed* and *Suz12*), PRC1 (*Bmi1*, *Ring1* and *Rnf2*) and H3K27 demethylases (*Kdm6a* and *Kdm6b*) were not altered by exposure to DSS-induced colitis (Figure 3B). These results indicated that aberrant H3K27me3 was induced at an early stage of colitis, and remained for the long term even after its inducer, inflammation, disappeared.

Altered H3K27me3 levels were associated with altered gene expression

The association between the altered H3K27me3 levels and altered gene expression was examined by temporal analysis of gene expression in colonic epithelial cells. Genes with increased H3K27me3 levels, *Dapk1* (gene body), *Gramd1b* (gene body), *Hdac5* (gene body), *Tbc1d16* (gene body) and *Zfpm1* (promoter), had decreased gene expression (Figure 4A). Among these genes, *Dapk1*, *Gramd1b* and *Tbc1d16* expression decreased at 5 weeks, but *Hdac5* and *Zfpm1* expression decreased at late phases of colitis. In contrast, genes with decreased H3K27me3 levels, *B4galnt1* (gene body), *Pdx1* (gene body) and *Plcd3* (gene body), had increased gene expression at 2 weeks (Figure 4B). These results indicated that altered H3K27me3 levels were associated with altered gene expression.

Some of the aberrant H3K27me3 were present in DSS-induced tumors

Alterations functionally involved in carcinogenesis are probably present also in tumor tissues. Therefore, we examined alterations of the H3K27me3 levels in colon tumors induced by azoxymethane and

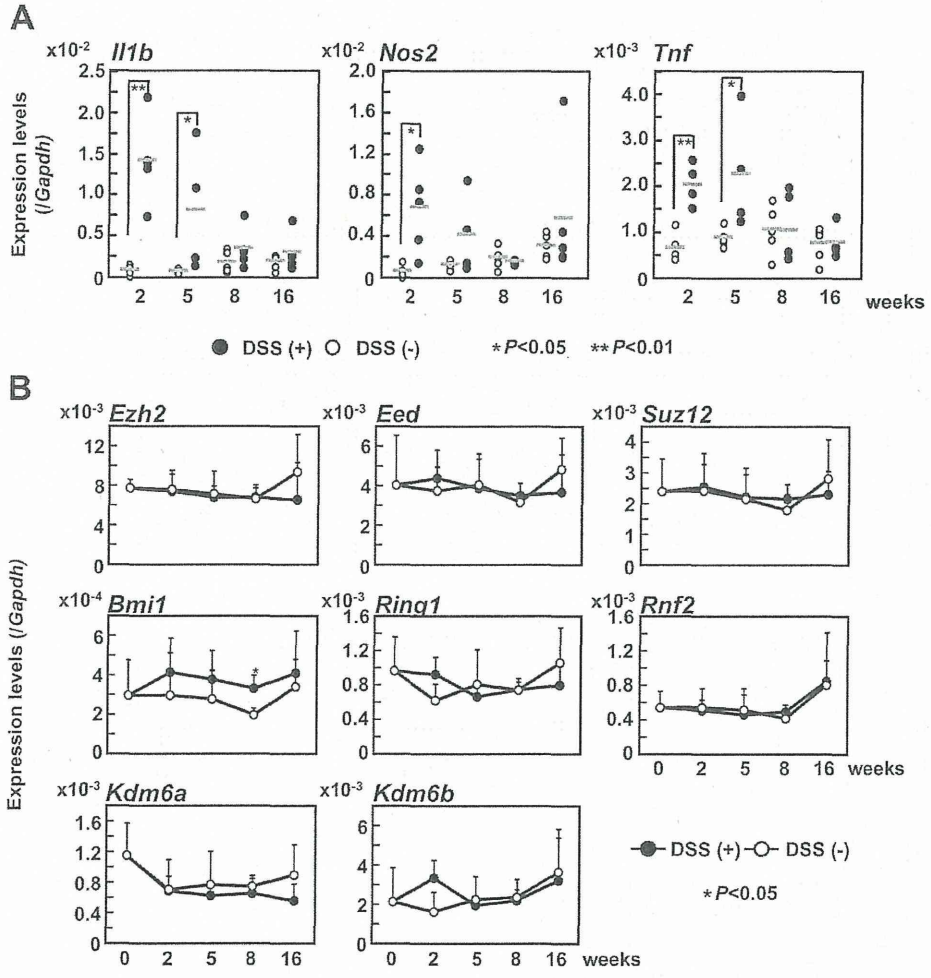

Fig. 3. Temporal profiles of expression of inflammation-related genes and polycomb-related genes in the course of DSS-induced colitis. (**A**) Temporal profiles of expression of inflammation-related genes. Gene expression was analyzed in samples of the entire colon by qRT-PCR. *Il1b*, *Nos2* and *Tnf* were upregulated at 2 and 5 weeks, but the upregulation disappeared at 8 and 16 weeks. Black and white circles show DSS-treated ($n = 5$) and mock-treated ($n = 5$) groups, respectively. The significance of difference was evaluated by the Mann–Whitney *U*-test (*$P < 0.05$, **$P<0.01$). (**B**) Temporal profiles of expression of polycomb-related genes. Gene expression was analyzed in colonic epithelial cells by qRT-PCR. Expression levels of these genes were not altered by exposure to DSS-induced colitis.

DSS. *Dapk1* and *Gramd1b* showed higher levels in colon tumors than those in mock-treated normal colonic epithelial cells whereas *Abca1*, *Hdac5*, *Tbc1d16* and *Zfpm1* did not. On the other hand, *B4galnt1* (CGI2300), ENSMUST00000065084.1, *Pdx1* and *Plcd3* showed lower levels in colon tumors than those in mock-treated normal colonic epithelial cells (Figure 5). These results suggested that some of the aberrant H3K27me3 induced in colonic epithelial cells was functionally involved in colon carcinogenesis.

Acquired H3K27me3 was followed by aberrant DNA methylation

A role of acquired H3K27me3 as a pre-mark for induction of aberrant DNA methylation was examined by analyzing DNA methylation levels of *Abca1*, *Dapk1*, *Gramd1b*, *Hdac5*, *Tbc1d16* and *Zfpm1* in FACS-purified colonic epithelial cells of mice 34 weeks after the initiation of DSS treatment. Among the six regions analyzed, *Dapk1* showed an increased DNA methylation level in colonic epithelial cells exposed to colitis (Figure 6). Two regions, *Hdac5* and *Tbc1d16*, showed high DNA methylation levels even in the mock-treated group, and methylation levels decreased by colitis. Three other regions, *Abca1*, *Gramd1b* and *Zfpm1*, were unmethylated in both groups. This result indicated that acquired H3K27me3 could function as a pre-mark for aberrant DNA methylation as pre-existing H3K27me3.

Discussion

In this study, we showed that aberrant H3K27me3 could be induced *in vivo* by exposure to a specific environment, here DSS-induced colitis, for the first time. The alterations of the H3K27me3 levels were probably involved in the formation of a field defect, and indicated to function as a pre-mark for induction of aberrant DNA methylation.

The involvement of the aberrant H3K27me3 in the field defect was indicated by the association between the altered H3K27me3 levels and altered gene expression, its persistence even after the disappearance of colitis and the presence of the alterations of H3K27me3 levels in colon tumors. If the alterations of the H3K27me3 levels are simple passengers, they are expected to be present in cancer tissues simply according to the frequency in non-cancer tissues. Nevertheless, such alterations were frequently present in tumors, and this indicated that the H3K27me3 alterations were functionally involved in carcinogenesis. Indeed, among the genes with increased H3K27me3 levels and frequently present in tumors, *Dapk1* is known as a positive mediator of apoptosis (31), and downregulated in various hematologic malignancies (32–34). Therefore, it is suggested that aberrant H3K27me3 induced by exposure to a specific inducer in normal-appearing tissues is involved in the formation of a field defect.

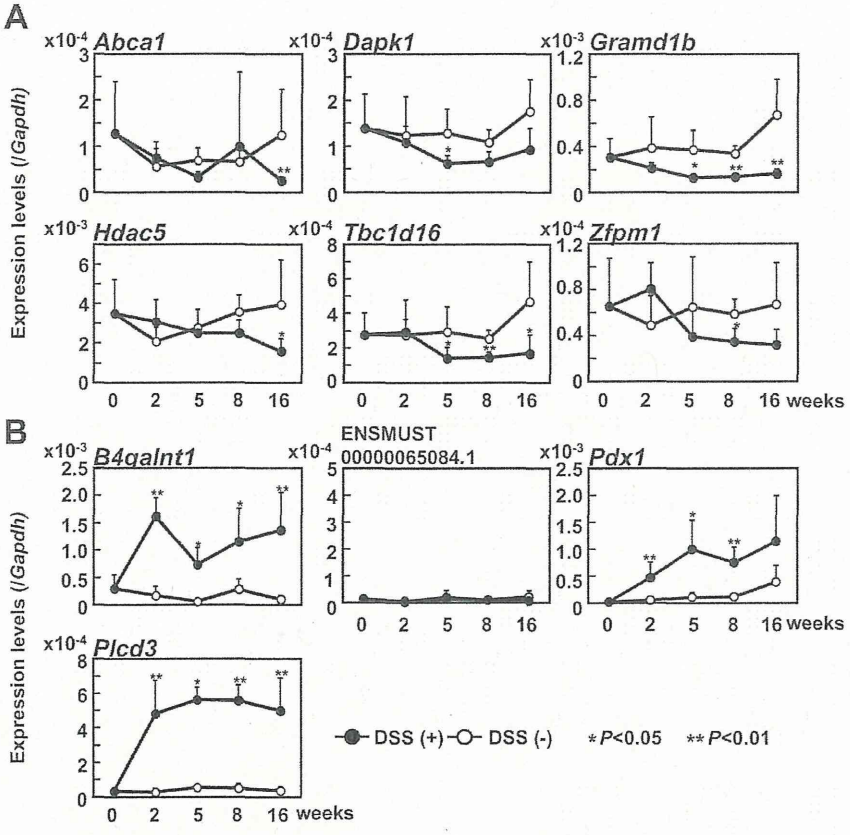

Fig. 4. Association between altered H3K27me3 levels and altered gene expression. (A) Temporal profiles of expression of genes with increased H3K27me3 levels. Gene expression was analyzed in colonic epithelial cells by qRT-PCR. *Dapk1*, *Gramd1b*, and *Tbc1d16* expression decreased at five weeks, but *Hdac5* and *Zfpm1* expression decreased at late phases of colitis. Black and white circles show DSS-treated ($n = 5$) and mock-treated ($n = 5$) groups, respectively. The significance of difference was evaluated by the Mann–Whitney *U*-test (*$P < 0.05$, **$P < 0.01$). (B) Temporal profiles of expression of genes with decreased H3K27me3 levels. *B4galnt1*, *Pdx1*, and *Plcd3* had increased expression at 2 weeks.

To prove the involvement of aberrant H3K27me3 in the formation of a field defect, intervention using specific inhibitors of histone H3K27 methyltransferase, Ezh2, and demethylases, Kdm6a and Kdm6b, is expected to provide important information. However, although 3-deazaneplanocin A (DZNep) is used for the inhibition of H3K27me3, it also affects other histone modifications such as H3K4me3 and H3K9me2 (35). Therefore, the precise role of aberrant H3K27me3 in the formation of a field defect cannot be assessed at this moment, and should be assessed once specific inhibitors of these enzymes are developed.

Acquired H3K27me3 at *Dapk1* also was indicated to function as a pre-mark for induction of aberrant DNA methylation. Although most of the methylated genes in cancer cells have H3K27me3 in normal cells (19–24,36), a small fraction of genes, including tumor-suppressor genes, are methylated in cancer cells despite the absence of H3K27me3 in normal cells (37). H3K27me3 levels of *Dapk1*, known as a tumor-suppressor gene, were increased by exposure to inflammation, and then aberrant DNA methylation was induced. Therefore, acquisition of a pre-mark, H3K27me3 by environmental exposure might be one of the mechanisms how aberrant DNA methylation is induced in tumor-suppressor genes that originally do not have the pre-mark, in addition to the mechanism of selection of rare events due to the growth advantage conferred (4).

Hdac5 showed a decrease in DNA methylation level despite its increase in the H3K27me3 level by DSS-induced colitis. Different from *Dapk1*, DNA methylation level was originally high at *Hdac5*. Generally, at regions whose DNA methylation level is originally high, H3K27me3 levels are increased after the removal of DNA methylation (38) due to the inhibitory effect of DNA methylation on the PRC2 recruitment (39). Therefore, it is possible that the decrease in DNA methylation level at *Hdac5* promoted the recruitment of PRC2, and led to the increase in the H3K27me3 levels.

As for the mechanisms of aberrant H3K27me3 induction, dysfunction of genes involved in the regulation of H3K27me3 can be considered. EZH2 is known to be upregulated in various human cancers including bladder, breast, gastric and prostate cancers, and these upregulations are known to be associated with poor prognosis (40–43). However, contrary to expectations, expression levels of genes involved in the regulation of H3K27me3 were not altered by exposure to DSS-induced colitis. Therefore, it is possible that localization or enzymatic activities of these factors are altered by exposure to DSS-induced colitis, and these alterations might be involved in aberrant H3K27me3 induction in colonic epithelial cells.

As for the mechanisms of persistence of aberrant H3K27me3 even after the disappearance of DSS-induced colitis, the maintenance mechanism of H3K27me3 by EZH2 (44,45) is probably involved. Namely, EZH2 at a replication site binds to H3K27me3 and introduces methyl groups to newly recruited histones. This maintenance mechanism in stem cells that can produce progenitor or differentiated cells seems to be involved in the persistence of aberrant H3K27me3 found here.

Alterations of other repressive histone modifications such as H3K9me2 and H3K9me3 were also induced in colonic epithelial cells by exposure to DSS-induced colitis, and regions with those alterations hardly overlapped with regions with H3K27me3-level alterations. Therefore, alterations of these repressive histone modifications

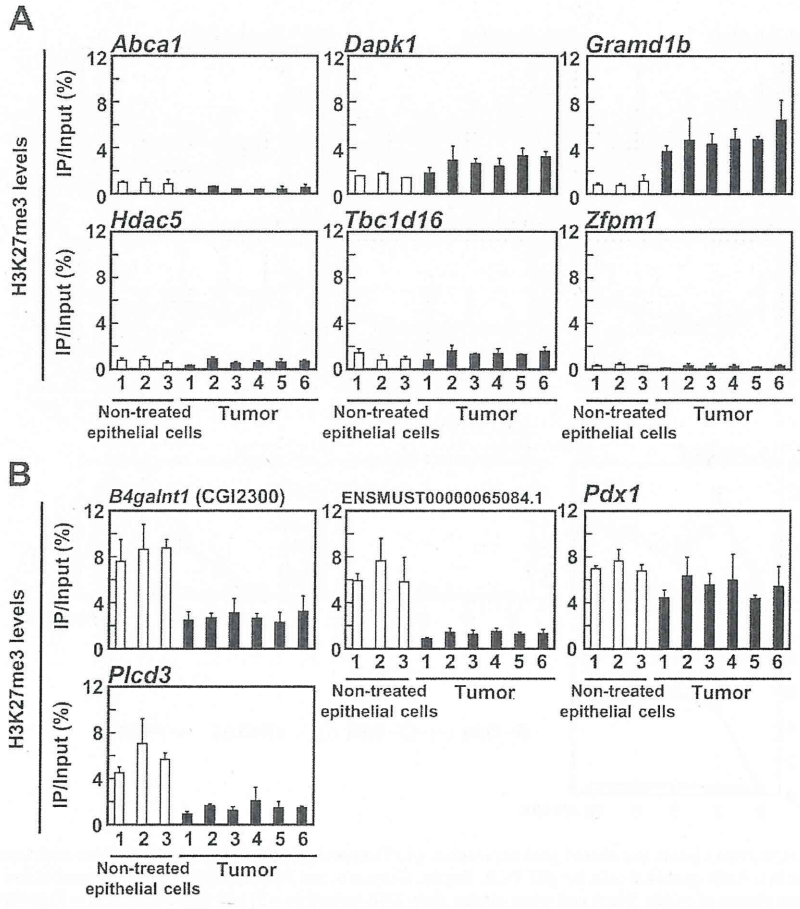

Fig. 5. H3K27me3 levels in colon tumors and age-matched normal colonic epithelial cells (non-treated). *Dapk1* and *Gramd1b* frequently showed high H3K27me3 levels in colon tumors (**A**), and *B4galnt1* (CGI2300), ENSMUST00000065084.1, *Pdx1* and *Plcd3* frequently showed low H3K27me3 levels in colon tumors (**B**). The frequent carryover of the altered H3K27me3 levels into tumors suggested that these alterations were functionally involved in tumor development. Error bars represent the experimental errors.

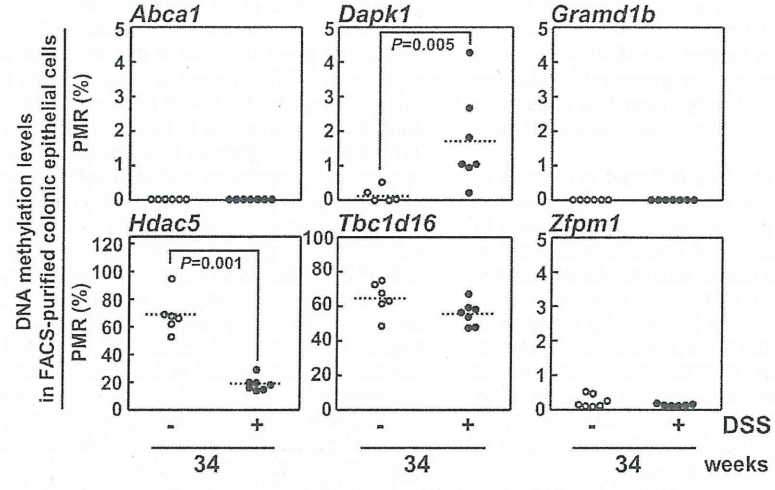

Fig. 6. DNA methylation analysis of genes with acquired H3K27me3. DNA methylation levels were analyzed by quantitative methylation-specific PCR in FACS-purified colonic epithelial cells. *Dapk1* showed increased DNA methylation levels in the DSS-treated group, indicating acquired H3K27me3 functioned as a pre-mark of DNA methylation induction. Black and white circles show DSS-treated ($n = 7$) and mock-treated ($n = 6$) groups, respectively. The significance of difference was evaluated by the Mann–Whitney *U*-test. Note that scales of the longitudinal axes are different for *Hdac5* and *Tbc1d16* from the others. PMR, the percentage of methylation reference.

might be involved in the formation of a field defect, independently of aberrant H3K27me3. However, in contrast with H3K27me3, the individual roles of H3K9me2 and H3K9me3 in repression of tumor-suppressor genes are not well understood due to their colocalization with DNA methylation (46), and assessment of their roles in the formation of a field defect seems difficult.

In conclusion, aberrant H3K27me3 was shown to be induced in normal-appearing tissues by exposure to a specific inducer, and its involvement in the formation of a field defect was suggested.

Supplementary material

Supplementary Tables 1–4 and Figures 1–4 can be found at http://carcin.oxfordjournals.org/

Funding

Grants-in-Aid for the Third-Term Comprehensive Cancer Control Strategy from the Ministry of Health, Labour and Welfare, Japan H20-2; Global Research Laboratory Program from Korea Foundation for International Cooperation of Science and Technology.

Conflict of Interest Statement: None declared.

References

1. Nakajima,T. *et al.* (2006) Higher methylation levels in gastric mucosae significantly correlate with higher risk of gastric cancers. *Cancer Epidemiol. Biomarkers Prev.*, **15**, 2317–2321.
2. Braakhuis,B.J. *et al.* (2003) A genetic explanation of Slaughter's concept of field cancerization: evidence and clinical implications. *Cancer Res.*, **63**, 1727–1730.
3. Ushijima,T. (2007) Epigenetic field for cancerization. *J. Biochem. Mol. Biol.*, **40**, 142–150.
4. Ushijima,T. *et al.* (2010) Aberrant DNA methylation in contrast with mutations. *Cancer Sci.*, **101**, 300–305.
5. Issa,J.P. *et al.* (1994) Methylation of the oestrogen receptor CpG island links ageing and neoplasia in human colon. *Nat. Genet.*, **7**, 536–540.
6. Maegawa,S. *et al.* (2010) Widespread and tissue specific age-related DNA methylation changes in mice. *Genome Res.*, **20**, 332–340.
7. Rakyan,V.K. *et al.* (2010) Human aging-associated DNA hypermethylation occurs preferentially at bivalent chromatin domains. *Genome Res.*, **20**, 434–439.
8. Li,X. *et al.* (2004) p16INK4A hypermethylation is associated with hepatitis virus infection, age, and gender in hepatocellular carcinoma. *Clin. Cancer Res.*, **10**, 7484–7489.
9. Maekita,T. *et al.* (2006) High levels of aberrant DNA methylation in Helicobacter pylori-infected gastric mucosae and its possible association with gastric cancer risk. *Clin. Cancer Res.*, **12**(3 Pt 1), 989–995.
10. Nakajima,T. *et al.* (2009) The presence of a methylation fingerprint of Helicobacter pylori infection in human gastric mucosae. *Int. J. Cancer*, **124**, 905–910.
11. Cedar,H. *et al.* (2009) Linking DNA methylation and histone modification: patterns and paradigms. *Nat. Rev. Genet.*, **10**, 295–304.
12. Kouzarides,T. (2007) Chromatin modifications and their function. *Cell*, **128**, 693–705.
13. Li,B. *et al.* (2007) The role of chromatin during transcription. *Cell*, **128**, 707–719.
14. Kondo,Y. *et al.* (2008) Gene silencing in cancer by histone H3 lysine 27 trimethylation independent of promoter DNA methylation. *Nat. Genet.*, **40**, 741–750.
15. Enroth,S. *et al.* (2011) Cancer associated epigenetic transitions identified by genome-wide histone methylation binding profiles in human colorectal cancer samples and paired normal mucosa. *BMC Cancer*, **11**, 450.
16. Gal-Yam,E.N. *et al.* (2008) Frequent switching of Polycomb repressive marks and DNA hypermethylation in the PC3 prostate cancer cell line. *Proc. Natl. Acad. Sci. U.S.A.*, **105**, 12979–12984.
17. Fujii,S. *et al.* (2008) Enhancer of zeste homologue 2 (EZH2) down-regulates RUNX3 by increasing histone H3 methylation. *J. Biol. Chem.*, **283**, 17324–17332.
18. Fujii,S. *et al.* (2008) Enhancer of zeste homolog 2 downregulates E-cadherin by mediating histone H3 methylation in gastric cancer cells. *Cancer Sci.*, **99**, 738–746.
19. Hahn,M.A. *et al.* (2008) Methylation of polycomb target genes in intestinal cancer is mediated by inflammation. *Cancer Res.*, **68**, 10280–10289.
20. McCabe,M.T. *et al.* (2009) A multifactorial signature of DNA sequence and polycomb binding predicts aberrant CpG island methylation. *Cancer Res.*, **69**, 282–291.
21. Ohm,J.E. *et al.* (2007) A stem cell-like chromatin pattern may predispose tumor suppressor genes to DNA hypermethylation and heritable silencing. *Nat. Genet.*, **39**, 237–242.
22. Schlesinger,Y. *et al.* (2007) Polycomb-mediated methylation on Lys27 of histone H3 pre-marks genes for de novo methylation in cancer. *Nat. Genet.*, **39**, 232–236.
23. Takeshima,H. *et al.* (2009) The presence of RNA polymerase II, active or stalled, predicts epigenetic fate of promoter CpG islands. *Genome Res.*, **19**, 1974–1982.
24. Widschwendter,M. *et al.* (2007) Epigenetic stem cell signature in cancer. *Nat. Genet.*, **39**, 157–158.
25. Li,Q. *et al.* (2009) Alterations of histone modifications by cobalt compounds. *Carcinogenesis*, **30**, 1243–1251.
26. Liu,F. *et al.* (2010) Epigenomic alterations and gene expression profiles in respiratory epithelia exposed to cigarette smoke condensate. *Oncogene*, **29**, 3650–3664.
27. Katsurano,M. *et al.* (2012) Early-stage formation of an epigenetic field defect in a mouse colitis model, and non-essential roles of T- and B-cells in DNA methylation induction. *Oncogene*, **31**, 342–351.
28. Takeshima,H. *et al.* (2011) Effects of genome architecture and epigenetic factors on susceptibility of promoter CpG islands to aberrant DNA methylation induction. *Genomics*, **98**, 182–188.
29. Yamashita,S. *et al.* (2006) Chemical genomic screening for methylation-silenced genes in gastric cancer cell lines using 5-aza-2'-deoxycytidine treatment and oligonucleotide microarray. *Cancer Sci.*, **97**, 64–71.
30. Niwa,T. *et al.* (2010) Inflammatory processes triggered by Helicobacter pylori infection cause aberrant DNA methylation in gastric epithelial cells. *Cancer Res.*, **70**, 1430–1440.
31. Deiss,L.P. *et al.* (1995) Identification of a novel serine/threonine kinase and a novel 15-kD protein as potential mediators of the gamma interferon-induced cell death. *Genes Dev.*, **9**, 15–30.
32. Claus,R. *et al.* (2012) Quantitative analyses of DAPK1 methylation in AML and MDS. *Int. J. Cancer*, **131**, E138–E142.
33. Qian,J. *et al.* (2009) Aberrant methylation of the death-associated protein kinase 1 (DAPK1) CpG island in chronic myeloid leukemia. *Eur. J. Haematol.*, **82**, 119–123.
34. Raval,A. *et al.* (2007) Downregulation of death-associated protein kinase 1 (DAPK1) in chronic lymphocytic leukemia. *Cell*, **129**, 879–890.
35. Miranda,T.B. *et al.* (2009) DZNep is a global histone methylation inhibitor that reactivates developmental genes not silenced by DNA methylation. *Mol. Cancer Ther.*, **8**, 1579–1588.
36. Takeshima,H. *et al.* (2010) Methylation destiny: Moira takes account of histones and RNA polymerase II. *Epigenetics*, **5**, 89–95.
37. Kikuyama,M. *et al.* (2012) Development of a novel approach, the epigenome-based outlier approach, to identify tumor-suppressor genes silenced by aberrant DNA methylation. *Cancer Lett.*, **322**, 204–212.
38. Brinkman,A.B. *et al.* (2012) Sequential ChIP-bisulfite sequencing enables direct genome-scale investigation of chromatin and DNA methylation cross-talk. *Genome Res.*, **22**, 1128–1138.
39. Bartke,T. *et al.* (2010) Nucleosome-interacting proteins regulated by DNA and histone methylation. *Cell*, **143**, 470–484.
40. Kleer,C.G. *et al.* (2003) EZH2 is a marker of aggressive breast cancer and promotes neoplastic transformation of breast epithelial cells. *Proc. Natl. Acad. Sci. U.S.A.*, **100**, 11606–11611.
41. Matsukawa,Y. *et al.* (2006) Expression of the enhancer of zeste homolog 2 is correlated with poor prognosis in human gastric cancer. *Cancer Sci.*, **97**, 484–491.
42. Raman,J.D. *et al.* (2005) Increased expression of the polycomb group gene, EZH2, in transitional cell carcinoma of the bladder. *Clin. Cancer Res.*, **11**, 8570–8576.
43. Varambally,S. *et al.* (2002) The polycomb group protein EZH2 is involved in progression of prostate cancer. *Nature*, **419**, 624–629.
44. Hansen,K.H. *et al.* (2009) Epigenetic inheritance through self-recruitment of the polycomb repressive complex 2. *Epigenetics*, **4**, 133–138.
45. Hansen,K.H. *et al.* (2008) A model for transmission of the H3K27me3 epigenetic mark. *Nat. Cell Biol.*, **10**, 1291–1300.
46. Kondo,Y. *et al.* (2004) Chromatin immunoprecipitation microarrays for identification of genes silenced by histone H3 lysine 9 methylation. *Proc. Natl. Acad. Sci. U.S.A.*, **101**, 7398–7403.

Received June 21, 2012; revised August 18, 2012; accepted September 9, 2012

HEPATOLOGY
Official Journal of the American Association for the Study of Liver Diseases

Role of Transcriptional and Posttranscriptional Regulation of Methionine Adenosyltransferases in Liver Cancer Progression

Maddalena Frau,[1] Maria L. Tomasi,[1] Maria M. Simile,[1] Maria I. Demartis,[1] Fabiana Salis,[1] Gavinella Latte,[1] Diego F. Calvisi,[1] Maria A. Seddaiu,[1] Lucia Daino,[1] Claudio F. Feo,[2] Stefania Brozzetti,[3] Giuliana Solinas,[4] Satoshi Yamashita,[5] Toshikazu Ushijima,[5] Francesco Feo,[1] and Rosa M. Pascale[1]

Down-regulation of the liver-specific *MAT1A* gene, encoding S-adenosylmethionine (SAM) synthesizing isozymes MATI/III, and up-regulation of widely expressed *MAT2A*, encoding MATII isozyme, known as *MAT1A:MAT2A* switch, occurs in hepatocellular carcinoma (HCC). Here we found *Mat1A:Mat2A* switch and low SAM levels, associated with CpG hypermethylation and histone H4 deacetylation of *Mat1A* promoter, and prevalent CpG hypomethylation and histone H4 acetylation in *Mat2A* promoter of fast-growing HCC of F344 rats, genetically susceptible to hepatocarcinogenesis. In HCC of genetically resistant BN rats, very low changes in the *Mat1A:Mat2A* ratio, CpG methylation, and histone H4 acetylation occurred. The highest *MAT1A* promoter hypermethylation and *MAT2A* promoter hypomethylation occurred in human HCC with poorer prognosis. Furthermore, levels of AUF1 protein, which destabilizes *MAT1A* messenger RNA (mRNA), Mat1A-AUF1 ribonucleoprotein, HuR protein, which stabilizes *MAT2A* mRNA, and Mat2A-HuR ribonucleoprotein sharply increased in F344 and human HCC, and underwent low/no increase in BN HCC. In human HCC, *Mat1A:MAT2A* expression and MATI/III:MATII activity ratios correlated negatively with cell proliferation and genomic instability, and positively with apoptosis and DNA methylation. Noticeably, the MATI/III:MATII ratio strongly predicted patient survival length. Forced *MAT1A* overexpression in HepG2 and HuH7 cells led to a rise in the SAM level, decreased cell proliferation, increased apoptosis, down-regulation of *Cyclin D1, E2F1, IKK, NF-κB*, and antiapoptotic *BCL2* and *XIAP* genes, and up-regulation of *BAX* and *BAK* proapoptotic genes. In conclusion, we found for the first time a post-transcriptional regulation of *MAT1A* and *MAT2A* by AUF1 and HuR in HCC. Low MATI/III:MATII ratio is a prognostic marker that contributes to determine a phenotype susceptible to HCC and patients' survival. *Conclusion*: Interference with cell cycle progression and I-kappa B kinase (IKK)/nuclear factor kappa B (NF-κB) signaling contributes to the antiproliferative and proapoptotic effect of high SAM levels in HCC. (HEPATOLOGY 2012;56:165-175)

Human hepatocellular carcinoma (HCC) is one of the most common and deadliest tumors worldwide.[1] Better understanding of the pathogenetic mechanisms may hasten identification of new prognostic markers and development of new diagnostic and therapeutic strategies.[1]

Molecular events leading to cell cycle deregulation in HCC include highest up-regulation of iNOS/

Abbreviations: AUF1, AUrich RNA binding factor 1; Chip, chromatin immunoprecipitation assay; COBRA, combined bisulfite restriction analysis; DN, dysplastic nodule; DUSP1, dual-specificity phosphatase 1; ERK, extracellular signal-regulated kinase; ERMA, enzymatic regional methylation assay; FOXM1, forkhead box M1B; FOXO1, forkhead box O1; GI, genome instability; HCC, hepatocellular carcinoma; HCCB, HCC with better prognosis; HCCP, HCC with poor prognosis; HuR, Hu-antigen R; iNOS, inducible nitric oxide synthase; MAT1A, methyl adenosyltransferase 1A; MeDip, methylated DNA immunoprecipitation; Mybl2, v-Myb avian myeloblastosis viral oncogene homolog-like2; qPCR, quantitative real-time reverse-transcription polymerase chain reaction; RAPD, random amplified polymorphic DNA; RASSF1A, Ras-associated factor 1; SAH, S-adenosyl-homocysteine; SAM, S-adenosyl-methionine; SL, surrounding nontumorous liver.

From the [1]Department of Clinical and Experimental Medicine, Division of Experimental Pathology and Oncology, University of Sassari, Sassari, Italy; [2]Department of Clinical and Experimental Medicine, Division of Surgery, University of Sassari, Sassari, Italy; [3]Department of Surgery "Pietro Valdoni," University of Rome "Sapienza," Rome, Italy; [4]Department of Biomedical Sciences, University of Sassari, Sassari, Italy; [5]National Cancer Center Research Institute, Tokyo, Japan.

Received September 9, 2011; accepted January 24, 2011.

NF-κB (inducible nitric oxide synthase/nuclear factor-κB)[2] and RAS/ERK (extracellular signal-regulated kinase) signaling, ubiquitination of ERK inhibitor DUSP1 (dual-specificity phosphatase 1),[3,4] and deregulation of FoxM1 (forkhead box M1B),[5] Mybl2 (v-Myb avian myeloblastosis viral oncogene homolog-like2),[6,7] and cell cycle key genes[8,9] in rapidly progressing HCC of F344 rats, genetically susceptible to hepatocarcinogenesis, and in a human HCC subtype with poorer prognosis (<3 years survival, after partial liver resection, HCCP). These changes were lower/absent in slow-progressing HCC of resistant BN rats and human HCC with better outcome (>3 years survival; HCCB). Furthermore, highest ubiquitination and proteasome degradation of cell cycle inhibitors of WAF/Kip families, P130, RASSF1A (Ras-associated factor 1), and FOXO1 (forkhead box O1) contribute to cell cycle up-regulation in F344 HCC and HCCP.[9,10]

SAM (S-adenosylmethionine) deficiency strongly influences HCC development. Low SAM content favors HCC development in rodents and humans,[11-15] whereas cell proliferation is inhibited by reconstitution of normal SAM levels in rat HCC, *in vivo*, by SAM administration,[11-13] and in human HCC cell lines by *MAT1A* (methionine adenosyltransferase 1A) transfection or SAM addition to culture medium.[14,16] In mammals the liver-specific *MAT1A* gene encodes MATI/III isozymes, whereas the widely expressed *MAT2A* encodes the MATII isozyme.[11] A fall in *MAT1A* expression with concomitant *MAT2A* up-regulation occurs in liver cirrhosis and HCC of rodents and humans.[11,17,18] The MATII isoform is inhibited by reaction product, and its up-regulation does not compensate for the fall in MATI/III isozymes.[11] Insights into the role of SAM deficiency in HCC pathogenesis were provided by HCC development in *MAT1A* knockout mice.[15]

Previous work[18] showed a role of deregulation of methionine metabolism in genome instability (GI) and aberrant DNA methylation in c-Myc transgenic mice and human HCC. The SAM/SAH (SAM/S-adenosylhomocysteine) ratio and liver MatI/III activity progressively decreased in dysplastic and neoplastic liver lesions of c-Myc transgenics and in most human HCC. This resulted in a rise of global DNA hypomethylation positively correlated with GI in mice and humans.[18] *Mat1A* down-regulation in cirrhotic liver of CCl_4-treated rats and in the human HepG2 cell line was associated with CCGG sequence methylation in the *Mat1A* promoter.[19] In Huh7 cells, *MAT1A* down-regulation was attributed to CCGG methylation at +10 and +80 of coding region.[20] *Mat2A* up-regulation in human HCC was associated with CCGG hypomethylation of the gene promoter.[21] Furthermore, recent work[22] showed *Mat1A* mRNA decrease in fetal rat liver, associated with an increase in its interaction with AUF1 (AUrich RNA binding factor 1), enhancing messenger RNA (mRNA) decay,[23] and an increase in *Mat2A* mRNA and its interaction with HuR (Hu-antigen R), which selectively binds to AUrich elements promoting mRNA stabilization.[23,24] Immunofluorescence analysis revealed increased HuR and AUF1 protein levels in human livers with HCC, suggesting post-transcriptional regulation of MAT proteins in HCC.[22]

These observations support the role of epigenetic regulation of MAT isozymes expression during HCC development. Here we tested if genetic susceptibility to HCC contributes to promoter methylation status and posttranscriptional deregulation of *Mat1A* and *Mat2A* during progression of rat hepatocarcinogenesis. Furthermore, because SAM levels influence cell proliferation, we investigated the prognostic role of *MAT1A:MAT2A* ratio and its contribution to the deregulation of signaling pathways involved in human HCC progression.

Materials and Methods

Animals and Treatments. F344 and BN rats were treated according to the "resistant hepatocyte" protocol.[25] Dysplastic nodules (DNs) and HCCs were collected at 32-40 and 50-67 weeks, respectively.

Human Tissue Samples. Six normal livers and 48 HCC and corresponding surrounding nontumorous

Supported by grants from the Associazione Italiana Ricerche sul Cancro (IG8952), Ministero Università e Ricerca (PRIN 2009), Regione Autonoma della Sardegna, Fondazione Banco di Sardegna; and a grant for the Third-term Comprehensive Cancer Control Strategy from the Ministry of Health, Labour, and Welfare, Japan.

Address reprint requests to: Rosa M. Pascale, Dipartimento di Medicina Clinica e Sperimentale e Oncologia, Sezione di Patologia Sperimentale e Oncologia, Università di Sassari, via P. Manzella 4, 07100 Sassari, Italy. E-mail: patsper@uniss.it; fax: 0039-079228485.

View this article online at wileyonlinelibrary.com.

DOI 10.1002/hep.25643

Potential conflict of interest: Nothing to report.

Additional Supporting Information may be found in the online version of this article.

livers (SLs) were used. Supporting Table S1 shows patient clinicopathological features.

Cell Lines and Treatments. Huh7 and HepG2 cell lines were transfected with *MAT1A* complementary DNA (cDNA) in pCMV6-XL expression vector (OriGene Technologies, Rockville, MD).

SAM, SAH, *and Global DNA Methylation Assays.* MatI/III and MatII activities and SAM and SAH levels[12] and global DNA methylation[26] were determined as reported.

Mat1A *and* MAT2a *Promoter Methylation.* Genomic DNA was digested with *HpaII* or MspI for Southern blot analysis. The samples were electrophoresed, transferred to a nylon membrane, and hybridized with a probe, generated by polymerase chain reaction (PCR) from liver gDNA. Bisulfite modified gDNA,[27] was used for combined bisulfite restriction analysis (COBRA),[28] methylation-specific PCR,[9] and enzymatic regional methylation assay (ERMA),[29] with the primers in Table S2.

Quantitative Real-Time Reverse Transcription (RT)-PCR (qPCR). qPCR reactions were performed as published.[3]

Chromatin Immunoprecipitation Assay (Chip). For Chip analysis,[31] chromatin extracted from nuclei was treated with anti-acetyl-histone H4 or rabbit IgG antibodies. Input DNA and immunoprecipitated chromatin were PCR-amplified with primers covering *Mat1a* and *Mat2A* gene promoters.

RNA Protein Interaction. Interaction of AUF1 and HuR proteins with *Mat1A* and *Mat2A* mRNAs, respectively, was determined by ribonucleoprotein immunoprecipitation in tissue extracts.[32]

Western Blot Analysis. Hepatic tissue samples were processed as reported.[5]

Random Amplified Polymorphic DNA (RAPD). Genomic alterations in human HCC were scored using 22 GC-rich arbitrary primers as described.[19]

Statistical Analysis. Differences of rat and human samples were analyzed by Tukey-Kramer, Student, or Mann-Whitney tests. Correlations were evaluated by multiple regression analysis, probability of overall survival by Mantel-Cox, and predictivity of patient survival by the Cox method.

See the Supporting Information for detailed descriptions of Materials and Methods.

Results

General Findings. Thirty-two to 40 weeks after initiation, high- and low-grade DNs developed in nine F344 and BN rats, respectively. At 50 weeks, seven moderately differentiated (ES grade II/III) and two poorly differentiated (ES grade IV) HCC developed in nine F344 rats. At 60-67 weeks, six moderately differentiated (ES grade II/III) and three well-differentiated (ES grade I/II) HCC developed in nine BN rats. Hematoxylin/eosin staining revealed the absence of contaminating normal parenchyma. DNs were distinguished from HCCs on the basis of histological criteria and for the presence of reticulin fibers and absence of glutathione synthase immunostaining[33] (not shown).

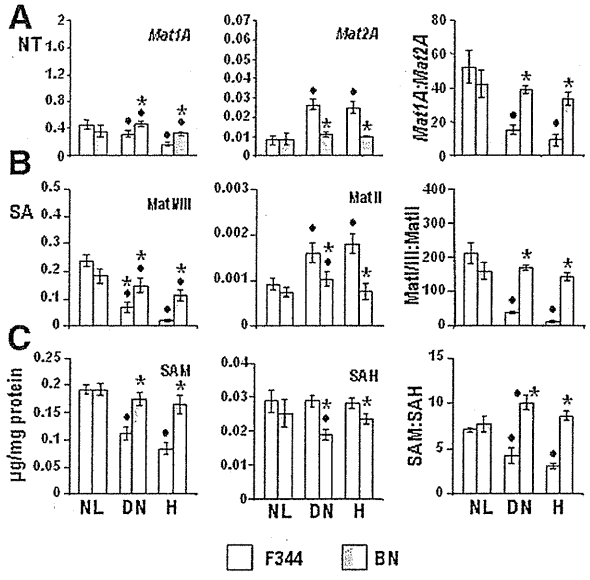

Fig. 1. *Mat1A* and *Mat2A* expression, MatI/III and MATII specific activity, and S-adenosylmethionine (SAM) and S-adenosylhomocysteine (SAH) content in normal liver (NL), dysplastic nodule (DN), and HCC (H) of F344 and BN rats. (A) Gene expression. The results are expressed as N-fold differences in target gene expression relative to the *RNR-18* expression, named N Target (NT). NT = $2^{-\Delta Ct}$, ΔCt of each sample was calculated by subtracting the Ct of the target gene from the Ct of the *RNR-18* gene. Enzymatic activity: (B) specific activity (SA) of MatI/III and MatII: nmol of labeled SAM/min, mg of protein. (C) SAM and SAH content and SAM/SAH ratio. Data are means ± standard deviation (SD) of six experiments. Analysis of variance (ANOVA): $P < 0.0001$ for gene expression, SA, and SAM and SAH content, and corresponding ratios. Tukey-Kramer test: (●) differences from control, at least $P < 0.05$. (*) F344 versus BN: at least $P < 0.05$.

Genetic Control of* Mat1A *and* Mat2A *Expression. No interstrain differences occurred in basic liver levels of *Mat1A* and *Mat2A* expression, MatI/III and MatII activities, and SAM/SAH ratio (Fig. 1). In F344 DN and HCC, *Mat1A* mRNA and MatI/III activity decreased, whereas *Mat2A* mRNA and MatII activity increased. In BN rat lesions, *Mat1A* level and MatI/III activity were higher, and *Mat2A* mRNA level and MatII activity were lower than in F344 rat lesions

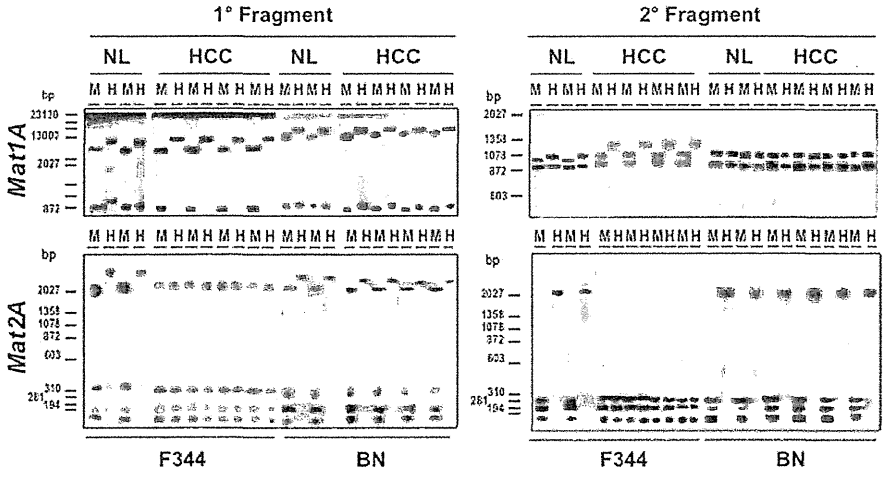

Fig. 2. Southern blot analysis of fragments I and II (cf. Fig. S1) of *Mat1A* and *Mat2A* promoter DNA, digested with *HpaII* (H), which is inhibited when the internal cytosine of CCGG sequence is methylated, or *MspI* (M), insensitive to methylation of the internal cytosine residue, in normal liver (NL) and HCC of F344 and BN rats. Note that digestion with *MspI* of *Mat1A* and *Mat2A* promoters of normal liver and HCC resulted in the same number and size of bands for both of F344 and BN rats. However, digestion of *Mat1A* promoter by *HpaII* only occurred in normal liver of both strains and in BN HCC. Digestion of *Mat2A* promoter by *HpaII* only occurred in F344 HCC. Southern blot hybridization was performed using labeled fragments of rat *Mat1A* and *Mat2A* promoters as described in Table S2.

(Fig. 1A,B). Accordingly, *Mat1A:Mat2A* and MatI/III: MatII ratios and SAM levels decreased in F344 liver lesions, and did not change significantly in BN DN and HCC (Fig. 1C). SAH level underwent low/no change in both strains and the SAM/SAH ratio decreased in F344 DN and HCC, and increased/did not change in BN rat lesions.

Mat1A *and* Mat2A *Promoter Methylation.* Because of the reported role of CCGG methylation in *MAT1A* and *Mat2A* promoters in rats and/or humans,[19-21] we evaluated the interstrain differences in methylation status of MAT genes. Southern analysis of *Mat1A* promoter indicated the presence of unmethylated CCGG sequences in normal liver of F344 and BN rats and HCC of BN rats, and of methylated sequences in F344 HCC (Fig. 2). Hypomethylated CCGG sequences occurred in two fragments of the *Mat2*A promoter of F344 HCC, corresponding to the −839, −791, −713, −622, and −401 positions, and to the −178, and +100 positions, respectively (Fig. S1). CCGG sequences in *Mat2*A promoter of normal liver of F344 and BN rats and BN HCC were methylated (Fig. 2).

According to COBRA, the TCGA sequence of *Mat1A* promoter at −1437 (site I; Fig. S1) was prevalently unmethylated in normal liver of both strains and in BN HCC, whereas it was partially methylated in F344 HCC. TCGA at −1385 (site II) was prevalently methylated in normal liver and HCC of both strains, with highest values in F344 HCC (Fig. S2). No differences in methylation of TCGA and CgCg sites of *Mat2A* promoter (Fig. S1) occurred between normal liver and HCC of both strains (not shown). No differences were found between normal liver and HCC of both strains for CpGs methylation in the −765:−458 fragment of *Mat1A* promoter, analyzed by msPCR, whereas hypomethylation of the −618:−405 CpGs of *Mat2A* promoter occurred in F344 HCC but not in BN HCC (Fig. S2).

CpGs methylation was also tested by ERMA (Fig. 3A). The analysis of three DNA fragments of *Mat1A* promoter, containing GpGs between −1205:−909, −778:−573, and −658:−242, respectively (Fig. S1), showed increased density of methylated CpGs in the first and third fragment of F344 HCC, and no change in BN HCC. The analysis of two DNA fragments of *Mat2A* promoter, with CpGs sites between −837:−333 and −439:+66, respectively (Fig. S1), evidenced hypomethylation of CpGs of F344 HCC, whereas no change and an increase in CpG islands methylation occurred in the first and second fragment of BN HCC, respectively (Fig. 3A). Because promoter fragments covering the transcription start site (Fig. S1) are the most important determinant of gene expression levels,[34] we further examined by methylated DNA immunoprecipitation (meDIP) the methylation of CpGs of Mat gene promoters close to ATG (−124:+10). No change in the methylation status of the single CpG in this fragment of *Mat1A* promoter occurred in either strain (not shown), whereas, in

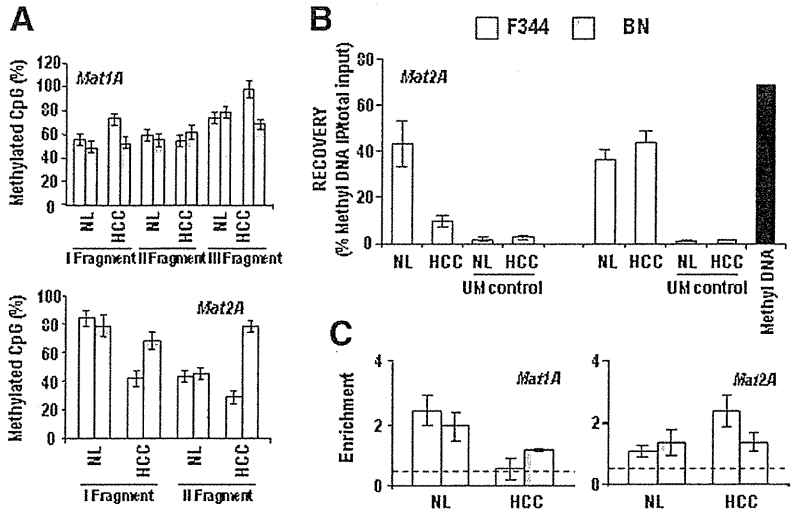

Fig. 3. Methylation status and histone H4 acetylation of *Mat1A* and *Mat2A* promoter in F344 and BN rats. (A) ERMA analysis of fragments I, II, and III of *Mat1A* promoter, and I and II of *Mat2A* promoter of normal liver (NL) and HCC of F344 and BN rats (cf. Fig. S1 and Table S1). Data are means ± SD of nine experiments. ANOVA: $P < 0.0001$ for *Mat1A* and *Mat2A*. Tukey-Kramer test: *Mat1A*, NL versus HCC, $P < 0.001$ for the first and third fragment, and third fragment of F344 and BN HCC, respectively. F344 versus BN, $P < 0.001$ for the first and third fragment. *Mat2A*, NL versus HCC, $P < 0.001$ for the first and second fragment, and the second fragment of F344 and BN HCC, respectively. F344 versus BN, $P < 0.001$ for the second fragment. (B) MeDip analysis of *Mat2A* between −124 and +10 basepairs. Recovery represents the efficiency of immunoprecipitated methyl DNA, calculated from qPCR data, and reported as percentage of the starting material: meDNA-IP/imput = $\hat{2}[Ct^{(input)} - Ct^{(meDNA\text{-}IP)} \times 100]$. Data are means ± SD of three independent determinations. ANOVA: $P < 0.0001$ for F344 an BN. Tukey-Kramer test: NL versus HCC for F344 $P < 0.001$. (C) Histone H4 acetylation. Chromatin immunoprecipitated by anti-acetyl-histone H4 antibody was amplified by PCR in the presence of primers covering the promoters of *Mat1a* and *Mat2A* genes. Negative controls with chromatin immunoprecipitated by anti-IgG antibody showed the absence of enrichment with respect to input. Results were normalized and presented as percentages of input DNA. The dashed line represents the threshold signal of 0.5%, above which significant enrichment for histone acetylation was scored. Data are means ± SD of three independent determinations. ANOVA: $P = 0.0015$ and $P = 0.0195$ for *Mat1A* and *Mat2A*, respectively. Tukey-Kramer test: HCC versus control (NL), *Mat1A*, $P < 0.001$ for F344 and BN; *Mat2A*, $P < 0.001$ for F344. F344 versus BN HCC, $P < 0.001$ for *Mat1A* and *Mat2A*.

agreement with ERMA analysis, an ≈5-fold decrease and no significant change of methyl-DNA recovery occurred in *Mat2A* promoter of F344 and BN rats HCC, respectively (Fig. 3B).

Due to the role of histone acetylation in the regulation of DNA methylation and gene expression,[31] we determined histone H4 acetylation in the core region of *Mat1A* and *Mat2A* promoters (Fig. 3C). No inter-strain difference in histone H4 acetylation of *Mat1A* and *Mat2A* promoters occurred in normal liver. The highest deacetylation of histone H4 occurred in *Mat1A* promoter of F344 HCC, compared with BN HCC. In *Mat2A* promoter the highest histone H4 acetylation was detected in F344 HCC and no change in BN HCC with respect to normal liver.

The above results document differences in Mat gene promoters methylation between HCCs differently prone to progress of F344 and BN rats. Evaluation of methylation status of MATs promoters (−370 to +100) in human HCCB and HCCP and corresponding SLs showed (Fig. S3) a 3.8 to 4.3-fold increase in MAT1A promoter methylation of SLP/HCCP, and no change in SLB/HCCB, compared with normal liver. MAT2A promoter methylation between −440 to −121 decreased 1.9 to 3-fold in both SLB/HCCB and SLP/HCCP. A significant decrease also occurred in HCCB, SLP, and HCCP between −121 and +100.

AUF1 and HuR Proteins Expression and Binding to Mat1A and Mat2A mRNAs. Recent work showed increased levels of HuR and AUF1 proteins in human livers with HCC,[22] suggesting posttranscriptional deregulation of MATs in human HCC. We evaluated this hypothesis by investigating Auf1 and HuR interactions with *MAT1A* and *MAT2A* mRNA, respectively, in rat and human HCC. A higher increase in AUF1 protein levels occurred in F344 than BN HCC, whereas HuR up-regulation only occurred in F344 HCC (Fig. 4A,B). Mat1A-AUF1 ribonucleoprotein (Fig. 4C) increased ≈10-fold and ≈2-fold, when compared with normal liver, in HCC of F344 and BN rats, respectively. Mat2A-HuR ribonucleoprotein increased ≈10-fold in F344 HCC and did not change in BN HCC. A progressive increase in AUF1 and HuR proteins and Mat1A-AUF1 and Mat2A-HuR

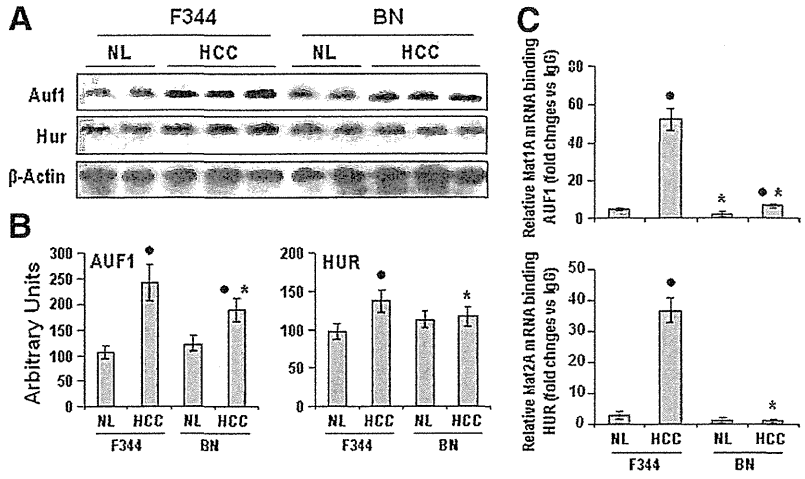

Fig. 4. Posttranscriptional regulation of Mats in normal liver (NL) and HCC of F344 and BN rats. (A) Representative western blot of Auf1 and HuR. (B) Chemiluminescence analysis showing the mean (SD) of three NL and five HCC from each strain. Optical densities of the peaks were normalized to β-actin values and expressed in arbitrary units. ANOVA: $P < 0.0001$ for AUF1, $P = 0.0047$ for HuR. Tukey-Kramer test: (●) HCC versus NL, $P < 0.001$ for AUF1, $P < 0.01$ for HuR. (*) BN versus F344, $P < 0.05$. for AUF1 and HuR. (C) Protein-mRNA complexes and IgG normal control were immunoprecipitated with specific antibodies and RNA was isolated and cDNA were analyzed by qPCR. Auf1- and HuR-ribonucleoproteins were calculated as fold changes versus control IgG. Data are means ± SD of three NL and five HCC from each strain. Tukey-Kramer test: (●) HCC versus NL $P < 0.001$; (*) BN versus F344, $P < 0.001$.

ribonucleoproteins occurred from human SL to HCC compared with normal liver (Fig. 5).

To further evaluate the contribution of promoter methylation and posttranscriptional control in the regulation of *MAT1A:MAT2A* ratio, we analyzed in Huh7 cells the effects of DNA hypomethylation and AUF1 knockdown on expression of *MAT1A*, whose sharp decrease is largely responsible for MAT1A:MAT2A switch. As shown in Fig. S4, a 3 to 9-fold decrease in promoter methylation, in 5-azacytidine-treated cells and a 1.6 to 2.5-fold decrease in AUF1 expression, induced by specific siRNA, are associated with a 6 to 9- and 2.2 to 3.5-fold rise in *MAT1A* expression, respectively. This indicates that both promoter methylation status and AUF1 expression may contribute to deregulation of *MAT1A* expression and the *MAT1A:MAT2A* ratio in HCC cells.

MatI/III Activity Correlates with Prognostic Parameters. The greatest decrease in *Mat1A:Mat2A* expression and MATI/III:MATII activity ratios in more aggressive F344 HCCs suggests that these parameters might both influence tumor progression and act as prognostic markers. To test this hypothesis, we analyzed the correlation of the MatI/III:MATII ratio with various progression-related features of rat and human HCC. Lower DNA synthesis and higher

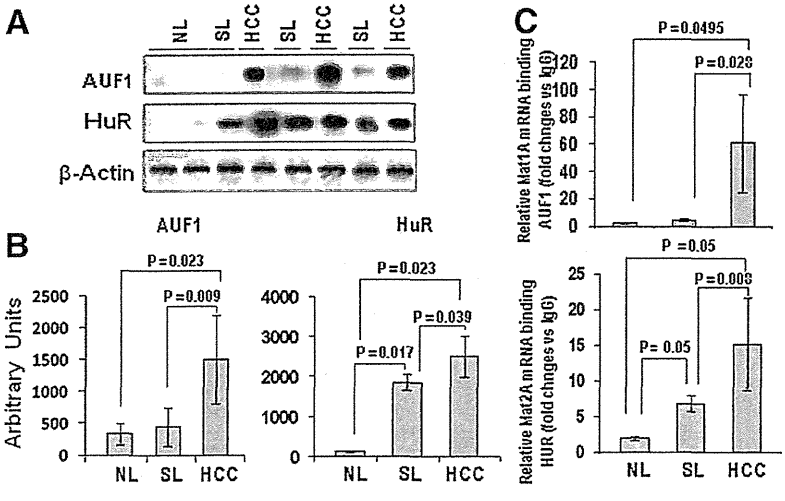

Fig. 5. Posttranscriptional regulation of Mats in human normal liver (NL), SL, and HCC. (A) Representative western blot of Auf1 and HuR. (B) Chemiluminescence analysis showing the mean ± SD of three NL and six HCC and corresponding SL. Optical densities of the peaks were normalized to β-actin values and expressed in arbitrary units. (C) Protein-mRNA complexes and IgG normal control were immunoprecipitated with specific antibodies and RNA was isolated and cDNA was analyzed by qPCR. Auf1- and HuR-ribonucleoproteins were calculated as fold changes versus control IgG. Data are means ± SD of three NL and six SL and HCC. Differences between means were calculated by Mann-Whitney test.

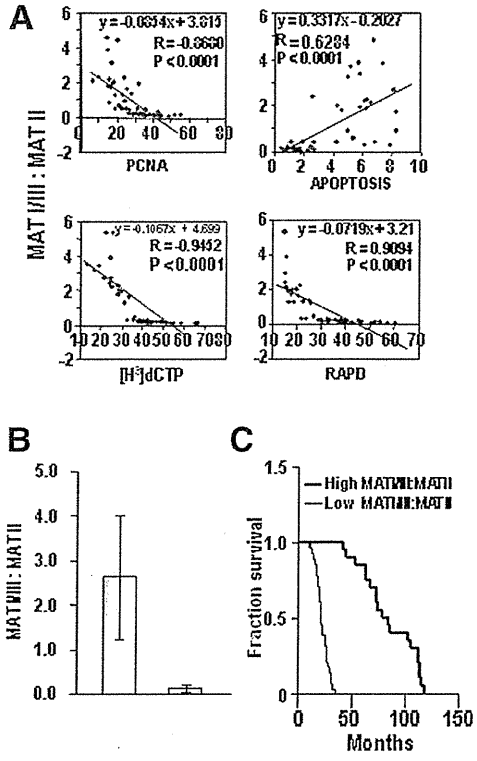

Fig. 6. (A) Relationships between MATI/III:MAT II ratio and proliferation index (expressed as the percentage of PCNA-positive nuclei with respect to total cells counted), apoptotic index (percentage of apoptotic cells), global DNA methylation (expressed as the amount of ^{3}H-dCTP in gDNA), and genomic instability (RAPD; expressed as the percentage of primers showing altered RAPD profiles). The values of ^{3}H-dCTP are inversely proportional to DNA methylation. Because of the nonparametric nature of the data, the Spearman rank correlation coefficient (R) was calculated. (B) MATI/III:MATII ratios in two distinct subgroups of human HCC with high (1.28-5.33) and low (0.029-0.42) ratios. Two-phase decay curves were used to calculate the cutoff value of MATI/III:MATII ratio (0.42-0.5) in correspondence to curve intersection in the correlation analysis of the ratio with PCNA, [H^3]dCTP, and RAPD. Difference between subgroups: Mann-Whitney test, $P < 0.0001$. (C) Kaplan-Meier survival curves of human HCC with high and low MATI/III:MATII ratios. Mantel-Cox statistical analysis: differences between survival curves MATI/III:MATII, $P < 0.0001$.

apoptosis occurred in BN rats DN and HCC than in F344 rat lesions, and methyl acceptance assay showed genomic hypomethylation in F344 DN and HCC but not in BN rat lesions (Fig. S5). The MATI/III:MATII ratio (Fig. S5) and *Mat1A:Mat2A* expression ratio (not shown) were negatively correlated with DNA synthesis and positively correlated with apoptosis of F334 and BN rat liver lesions. A negative correlation of the MATI/III:MATII ratio with [^{3}H]dCTP (Fig. S5) indicates its positive correlation with DNA methylation.

The analysis of 48 human HCCs (Fig. S6) showed a progressive decrease in *Mat1A* expression and MATI/III activity and progressive increase in *MAT2A* expression and MATII activity from SL to HCC as compared with normal liver values. These changes were paralleled by progressive increase in proliferation rate, and decrease in DNA methylation (increase in [^{3}H]*methyl* incorporation) from SL to HCC, compared with normal liver. Apoptotic index increased in SL and HCC (Figs. S6, S7). Correlation analysis revealed (Fig. 6A) an inverse correlation of *MAT1A:MAT2A* expression ratio (not shown) and MATI/III: MATII activity ratio with PCNA expression, [^{3}H]*methyl* incorporation into DNA, and GI, and a direct correlation with apoptosis. Notably, direct correlation of MATI/III:MATII ratio with the proliferation rate ($R = 0.6983$, $P < 0.0001$) and inverse correlation with DNA methylation ($R = 0.9056$; $P < 0.0001$) occurred in SL, whereas no significant correlation with apoptosis index was found.

The results in Fig. 6A clearly indicate the presence of two patient subgroups with significantly different MatI/III:MatII ratios (Fig. 6B) and survival length, with the HCC subset showing the lower MATI/III:MARII ratio being associated with shorter survival (Fig. 6C). Remarkably, Cox analysis showed that MATI/III:MATII ratio significantly predicted patient survival length: hazard ratio, 0.811, 95% confidence interval: 0.663-0.993, $P = 0.042$. In the multivariate analysis model (Table 1), the MATI/III:MATII ratio remained significantly associated with overall survival, together with patients' age, tumor etiology and grade, PCNA expression, DNA methylation, and GI. A significant association of the *MAT1A:MAT2A* expression ratio and etiology, PCNA, and GI with overall survival was also found (not shown).

Effects of* MAT1A *Overexpression in Human HCC Cell Lines. The above results suggest a role of high *MAT1A* expression and *MAT1A:MAT2A* ratio in

Table 1. Multivariate Analysis of Factors Contributing to Overall Survival

	Overall Survival		
Variable	Hazard Ratio	95% Confidence Interval	*P* Value
Sex	2.27	0.85-6.09	0.102
Age	0.96	0.92-1.00	**0.047**
Etiology	0.69	0.49-0.97	**0.031**
Cirrhosis	1.11	0.37-3.31	0.849
Tumor size	1.74	0.59-5.13	0.310
Edmondson-Steiner grade	2.83	1.07-7.50	**0.037**
AFP secretion	1.53	0.65-3.62	0.334
MATI/III:MATII ratio	0.76	0.62-0.94	**0.010**
PCNA	1.06	1.01-1.11	**0.011**
Apoptosis	1.08	0.75-1.55	0.697
Global DNA methylation	1.19	1.02-1.41	**0.032**
Genomic instability (RAPD)	1.22	1.09-1.37	**0.001**

AFP, α-Fetoprotein; PCNA, proliferating cell nuclear antigen; RAPD, random amplified polymorphic DNA.